ANGULAR DISTRIBUTIONS OF SOME γ-RAYS PRODUCED IN NUCLEAR REACTIONS

Thesis by

Robert Briggs Day

In Partial Fulfillment of the Requirements

For the Degree of

Doctor of Philosophy

California Institute of Technology

Pasadena, California

1951

ACKNOWLEDGMENTS

I wish to express my thanks to Dr. Joseph E. Perry, Jr., for his active cooperation in all phases of the experiments described here. His help was invaluable not only in the execution of the experiments but also in their planning and interpretation. The problems were suggested by Professors W. A. Fowler and R. F. Christy, who were also ready at all times with helpful advice and criticism.

I am indebted to Mr. R. G. Thomas for pointing out some of the fundamental ideas used in calculating angular distributions. Further discussions with him and with Professor Christy were very helpful in clarifying various questions that arose in the course of the calculations.

ABSTRACT

Measurement of the angular distributions of the γ-rays produced in nuclear reactions promises to be a fruitful method in helping to determine the spins and parities of the nuclear states involved. The methods and apparatus for doing this for proton reactions on light nuclei are described. Results are given for the following reactions: $F^{19}(p,\alpha\gamma)O^{16}$ at various resonances between 850 and 1400 kev, $C^{12}(p,\gamma)N^{13}$ at the 1696 kev resonance, and $C^{13}(p,\gamma)N^{14}$ at the 1754 kev resonance. A short account is given of the principles involved in the calculation of angular distributions. This is followed by a discussion of the experimental results in terms of the spins and parities of the states. For the fluorine reaction this has already been done by Chao. The $C^{12}(p,\gamma)N^{13}$ resonance seems to be due to a compound nucleus with spin 3/2 and even parity. For the $C^{13}(p,\gamma)N^{14}$ resonance the theory does not permit a definite assignment to be made on the basis of this experiment.

TABLE OF CONTENTS

I. INTRODUCTION

Among the important properties of the excited states of nuclei are spin or angular momentum, parity, energy, and width. In the past, most experiments in nuclear physics have been designed to yield information on the energy and width, but inferences concerning spin and parity have often rested on precarious ground. Recently, experiments have been performed on the angular distribution of the particles[1][2] or γ-rays[3][4] produced in nuclear reactions and on the angular correlation between successive particles or γ-rays[5 - 10]. Since the results of these experiments depend only on the spin and parity of the states involved and the relative orbital angular momentum of the particles they can advance our knowledge of nuclei considerably by giving direct information on these properties. It is true that the results of an experiment cannot always be interpreted unambiguously, but when considered in conjunction with other results they can often give conclusive answers.

The following two sections present the results of experiments measuring the angular distribution of the γ-rays produced by bombarding fluorine and carbon with protons. The last section discusses the theoretical interpretation of these results in terms of the spins and parities of the nuclear states involved.

II. METHOD AND APPARATUS

The γ-rays investigated here were produced in the following resonance reactions:

(1) $F^{19}(p,\alpha\gamma)O^{16}$ at various resonances from 850 to 1400 kev.
(2) $C^{12}(p,\gamma)N^{13}$ at the 1696 kev resonance.
(3) $C^{13}(p,\gamma)N^{14}$ at the 1754 kev resonance.

The protons initiating the reactions were accelerated in the 3 Mev electrostatic accelerator and analyzed in energy by a double-focusing magnet. The experimental arrangement of the target chamber and detecting equipment is shown in Figure 1. The adjustable horizontal slits determined the energy resolution

of the magnet, which varied from 0.1 to 0.3% depending on the intensity required.

The two sets of adjustable slits defined the size of the beam and aided in determining the direction of the beam. The target chamber was of aluminum, 3 3/4 inches in diameter with 1/32 inch walls. A projection on the bottom fitted into a lucite bushing, which in turn was inserted into a fixed brass tube that served as a bearing about which the counters rotated. At the back of the chamber, diametrically opposite the beam entrance tube, was a thin quartz window. This had vertical and horizontal scratches on it that were carefully made with reference to the axis of the chamber. By observing the position of the beam on this window and adjusting the position of the target chamber and counters as a unit, the beam could be made to pass quite accurately through the center of the chamber.

The target support consisted of a foil that was clamped or soldered to a thin frame attached to a piece of drill rod. This was constructed so that the face of the foil fell on the axis of the target chamber. In the $F^{19}(p,\alpha\gamma)O^{16}$ experiment the target was a thin layer of CaF_2 evaporated in vacuo on a .005" copper foil. For the $C^{12}(p,\gamma)N^{13}$ experiment the target was soot from a smoky benzene flame, collected on a .001" tantalum foil. The drill rod could be raised or lowered through an O-ring vacuum seal, thus permitting a fresh surface to be exposed to the beam when necessary. The target could also be rotated so that the absorption in the target support was minimized. In practice it was turned so that the target surface made an angle of 45° with the beam. In measuring the γ-ray intensity at angles from 0° to 90° the target was placed at that 45° position from which the γ-rays had to pass through the supporting foil to reach the detector. At angles above 90° the target was rotated through 90° so that the γ-rays passed only through the walls of the target chamber. A small correction was applied to the data obtained in this way. The angle of the target was set by means of a pointer attached to the drill rod and a protractor. The zero position was obtained by observing the reading when the shadow of the target support turned edgewise to the beam was narrowest. This setting was reproducible to within one-half degree.

In the $C^{12}(p,\gamma)N^{13}$ experiment the low intensity of the reaction required

that the counters be moved closer to the target. Therefore, we substituted a brass target chamber 5/8" in diameter, with 1/32" walls. Otherwise the details were the same.

The detector consisted of three Geiger counters mounted on an aluminum frame that could be rotated about the axis of the target chamber. The two back counters were connected in parallel and coincidences recorded between these and the front counter. By using two back counters the solid angle was increased without affecting the angular resolution appreciably, since this is determined principally by the angle subtended by the counters in the vertical direction. The Geiger counters used had a thin glass wall (30 mg/cm^2) with an effective volume 23/32" in diameter and 3 3/4" long. This was an average size and individual counters sometimes varied by 10% from this. The distance between the center of the front counter and the line of centers of the two back counters was 1 1/2", while the distance from the center of the front counter to the target could be set at either 1 1/2" or 3 13/16". Just in front of the first counter was an aluminum converter from 1/8" to 19/32" thick. Provision was made for inserting aluminum absorbers between the front and back counters. These were always held in place against the back counters. Finally the entire sides and back of the counter frame were covered with aluminum of 1/8" or 1/4" thickness to reduce the counting rate from scattered secondaries. This decreased the angular resolution slightly, but again the effect was slight since the vertical angle was the principal one in determining the resolution.

The Geiger counters were connected to a standard form of cathode-follower quench circuit. The output of these was amplified and sharpened in a pulse forming circuit and then fed into a coincidence circuit whose resolving time was five microseconds. The output of the quench circuit connected to the front counter was also fed into an amplifier and scaler so that it could be recorded independently.

In order to reduce the X-ray background produced by the electrostatic generator the target chamber and Geiger counters were both surrounded by a lead house two inches thick, whose inside dimensions were 14 1/2 x 14 1/2 x 10 inches. This was lined with 1/4 inch of aluminum to reduce the effects of scattering from the walls. In order to test the effect of the house on the apparatus, a ThC" source was inserted in the target chamber in the position usually occupied

by the target. The γ-ray intensity was then measured from 0° to 160° on both sides of the target chamber. This proved to be isotropic to within the statistical error of $\pm$ 2%, thus showing that no sources of anisotropy were being introduced by the method of measuring the angular distribution.

The method of obtaining the data was slightly different in the two experiments reported here. In both cases the target chamber was completely insulated from ground and the total beam charge striking the target measured by a current integrator, whose accuracy was about one percent. In addition, for the fluorine experiment a Geiger counter surrounded by .350" of aluminum was placed 3 1/2" from the target at 90° to the beam. This was used as a monitor and the angular distribution obtained by observing the ratio of coincidence counts to monitor counts as a function of the angle that the coincidence counter frame made with the beam. The number of monitor counts for a given amount of charge generally showed a tendency to decrease during the course of the measurements. This was due to the formation of a carbon layer on the surface of the target, which caused the effective proton energy to be somewhat less than the resonance energy. By increasing the proton energy slightly the monitor counting rate could be brought up to normal. Thus, the current integrator was used essentially as an aid in keeping the yield constant and served to monitor the effective proton energy.

In the carbon experiments no monitor counter was used, since its statistical error would have been several times greater than the integrator error. It was not necessary to use the integrator as a proton energy monitor because the targets were already of carbon many times thicker than the layers deposited during bombardment.

In designing the apparatus to measure the angular distribution of γ-rays produced in nuclear reactions there were a number of factors to be considered in order that the true distribution would not be distorted by extraneous effects.

These are listed below and then discussed in more detail with reference to their effect on the experiments.

(1) Scattered radiation

(2) Scattered secondary electrons

(3) Absorption of the γ-rays

(4) Background radiation

(5) Geometrical effects

(6) Counter resolution

(1) Scattered Radiation.

Because of the large background of X-rays from the electrostatic generator at high voltages it was necessary to surround the target chamber and detectors with a house of lead bricks two inches thick. This house then scattered γ-rays into the detector. However, this effect was eliminated by using two Geiger tubes in coincidence as a sort of telescope and placing enough aluminum between them to absorb low energy secondaries. Since large-angle Compton scattering degrades γ-ray energies to the order of 0.5 Mev, a detector of this type counts only γ-rays from the target. Some small-angle scattering, it is true, could occur in the walls of the target chamber or in the target support, but these were made thin to reduce the effect.

(2) Scattered Secondary Electrons.

Secondary electrons produced in a Compton or pair process might be scattered from the walls of the target chamber or lead house and be counted. By lining the house with 1/4" aluminum we greatly reduced the scattering from the latter. In addition, the Geiger counters were surrounded by 1/8" or 1/4" of aluminum depending on the experiment. After this, tests showed that the coincidence counting rate was not affected even when a large lead block was placed close to the counters.

(3) Absorption.

In our early experiments the γ-ray intensity at large angles was lower than we expected. At these angles the γ-rays had to pass obliquely through the wall of the beam tube in order to reach the detector and thus underwent a slightly greater absorption. This was corrected by redesigning the target chamber so that the γ-rays had to go through the same wall thickness at all angles.

At angles from 0 - 90 degrees with the beam the γ-rays were detected only after passing through the target backing, while at angles greater than 90 degrees they did not. A small correction, which was determined experimentally was made for this. This value also agreed with one calculated theoretically.

(4) Background.

The effect of X-rays produced by the Van de Graaff generator was made negligible by the lead shielding mentioned previously. However, in the $C^{12}(p,\gamma)N^{13}$ experiment the γ-rays produced by protons passing through the target and striking the tantalum target backing accounted for about 10% of the counting rate. By bombarding the clean back side of the tantalum, this contribution to the counting rate could be determined. It was always isotropic within the statistical error. There was also a soft component due to the annihilation of positrons from the decay of N^{13}. The secondary electrons from this γ-ray could be completely stopped by placing .030" of aluminum absorber between the Geiger counters, so that the coincidence rate was not affected.

Similarly, in the $F^{19}(p,\alpha\gamma)O^{16}$ experiment the nuclear pairs were strong enough to have affected the results. However, the combination of the aluminum shielding around the counters plus the absorber between them was always sufficient to prevent the pairs from producing coincidences, while the absorber between the counters ruled out the possibility of counts from annihilation radiation.

(5) Geometrical Effects

If the axis of rotation of the counters does not pass through the spot on the target that is bombarded by the beam, the distance from the target to the counters will vary as the counters are rotated. Consequently, terms in sin Θ or cos Θ will be introduced into the measured angular distribution. Thus, it is necessary to construct the target chamber and counter framework rather carefully, and then to see that the beam is aligned so that it strikes the target on center. By measuring the distributions on both sides of the beam and averaging them, one can remove to first order any errors produced by sidewise displacements of the beam from the counter axis of rotation, as well as any error in determining the direction of the beam, from which the angles are measured.

(6) Counter Resolution

The distance at which the counters were placed was limited by the requirement that the lead shielding not be too bulky as well as that the intensity be sufficient. At the relatively small target to counter distance required the angles subtended by the counters at the source were not negligible, particularly in the vertical direction. A correction can be made for this as follows: Assume that the effective area presented to the source by the counter arrangement is part of a cylinder of height 2b and radius ρ, subtending an angle 2α at the source. The axis of the cylinder passes through the source at right angles to the beam. Let Θ be the angle the center of this section makes with the beam and θ be the angle a γ-ray makes with the beam. Then if the true angular distribution is

$$1 + A \cos^2 \theta + B \cos^4 \theta$$

the angular distribution measured by the counters will be

$$I(\Theta) = \iint (1 + A \cos^2 \theta + B \cos^4 \theta)\, d\Omega$$

$$= \int_{-b}^{b} \int_{90-\theta-\alpha}^{90-\theta+\alpha} \left(1 + A \frac{\rho^2 \sin^2\phi}{Z^2+\rho^2} + B \frac{\rho^4 \sin^4\phi}{(Z^2+\rho^2)^2}\right) \frac{\rho^2 \, d\phi \, dZ}{(Z^2+\rho^2)^{3/2}}$$

$$= \frac{4b\alpha}{\sqrt{b^2+\rho^2}} \left\{1 + \frac{1}{2} A k(1-\xi) + A k \xi \cos^2\theta + \frac{1}{2} Bk' \left(\frac{3}{4} - \xi + \frac{1}{4}\xi'\right) + k'B(\xi - \xi')\cos^2\theta + k'B\xi' \cos^4\theta\right\}$$

$$= \frac{4b\alpha}{\sqrt{b^2+\rho^2}} \left[1 + \frac{1}{2} Ak(1-\xi) + \frac{1}{2} Bk'\left(\frac{3}{4} - \xi + \frac{1}{4}\xi'\right)\right] \quad x$$

$$1 + \frac{Ak\xi + Bk'(\xi - \xi')}{1 + \frac{1}{2} Ak(1-\xi) + \frac{1}{2} Bk'(\frac{3}{4} - \xi + \frac{1}{4}\xi')} \cos^2\theta + \frac{B k' \xi' \cos^4\theta}{1 + \frac{1}{2} Ak(1-\xi) + \frac{1}{2} Bk'(\frac{3}{4} - \xi + \frac{1}{4}\xi')}\Bigg]$$

where $k = \dfrac{1 + \frac{2}{3}\frac{b^2}{\rho^2}}{1 + \frac{b^2}{\rho^2}}$

$$k' = \frac{8b^4 + 20\, b^2\rho^2 + 15\rho^4}{15\,(b^2+\rho^2)^2}$$

$$\xi = \frac{\sin 2\alpha}{2\alpha}$$

$$\xi' = \frac{\sin 4\alpha}{4\alpha}$$

We see that the expressions multiplying $\cos^2\theta$ and $\cos^4\theta$ are the experimentally determined coefficients, A' and B', in terms of the true coefficients, A and B. Solving for A and B in terms of A' and B' we have

$$A = \frac{1}{D} \left\{A' k' \xi' - B' k' (\xi - \xi')\right\}$$

$$B = \frac{1}{D} \cdot B' k\xi$$

where

$$D = \left[k\xi - \frac{1}{2} A' k (1-\xi)\right] \left[k' \xi' - \frac{1}{2} B' k' \left(\frac{3}{4} - \xi + \frac{1}{4}\xi'\right)\right]$$

$$+ \left[k'(\xi - \xi') - \frac{1}{2} A' k' \left(\frac{3}{4} - \xi + \frac{1}{4} \xi'\right)\right] \left[\frac{1}{2} B' k(1 - \xi)\right]$$

For a coincidence counter arrangement the determination of α and $\frac{b}{o}$ is too complicated to calculate theoretically, hence these quantities were determined empirically using a well-collimated beam of γ-rays from ThC". For the counter arrangement used in the $F^{19}(p,\alpha\gamma)O^{16}$ experiment the above equations reduced to

$$A = \frac{1.03\ A' - .038B'}{.991 - .005A'}$$

$$B = \frac{1.417\ B'}{.991 - .005\ A'}$$

III. EXPERIMENTAL RESULTS

(1) $F^{19}(p,\alpha\gamma)O^{16}$

In all the work done on this reaction an aluminum converter 19/32" thick was used and a .150" thick aluminum absorber was placed between the coincidence counters. The center of the front counter was 3 13/16 inches from the target, which was a thin layer of CaF_2 evaporated in vacuo on a .005" copper foil. The target thickness was 10 kev at 873.5 kev. This was determined by measuring the experimental width at half-maximum (Γ') and using the relation

$$\xi^2 = \Gamma'^2 - \Gamma^2$$

where ξ is the target thickness and Γ the natural half-width. The value of used was 5.2 kev. as determined by Bennett et. al[11]. From time to time the target support was moved to expose a fresh surface to the proton beam. Measurements showed that the CaF_2 layer was uniform to within 10% over the area used.

The yield in this reaction has been investigated very thoroughly up to proton energies of about 1400 kev. Above this the only published work is that of Bernet, Herb, and Parkinson[12], who made measurements on the yield up to

2.2 Mev. However, their results on the yield were not very consistent. Accordingly, we measured the yield up to 2.7 Mev, using the same apparatus used in the angular distribution experiments. To obtain, in addition to the yield, an estimate of how the angular distribution varied with energy we placed the coincidence counters at 0° and the monitor counter at 90°. The ratio of the counts from these two then provides a measure of the angular distribution, assuming it is of the form $1 + a \cos^2\theta$, since $\frac{I(0)}{I(90^{\circ})} = 1 + a$. The results are shown in Figure 2. Maxima in the yield occur at 1.51, 1.71, 1.96, 2.04, 2.19, 2.32 and 2.64 Mev. It should be emphasized that this was only a preliminary survey with no attempt being made to measure the energies or yields precisely. Thus, the energy is known to about 10 - 15 kev. Since relatively large energy steps were taken at higher energies no narrow peaks would have been observed. However, the general nature of the curve indicates that the resonances are broad and overlapping. At higher energies the counting rate was not always reproducible within the statistical error; hence, maxima have been drawn in the curve only when shown by both the monitor and coincidence counters.

Angular distributions of the γ-rays were measured at a number of resonances between 873 kev and 1380 kev, plus two other energies of interest. These were obtained as described in the preceding section.

When the measurements were completed it was found that a small systematic asymmetry existed with respect to a plane perpendicular to the proton beam. Since the radiation involved here is from levels of a residual nucleus that are very narrow (of the order of electron volts) and presumably do not overlap, no such asymmetry should exist.* Half of the observed effect could be attributed to absorption in the target backing. The other half was presumably due to

---

* This is because terms in odd powers of $\cos\theta$ can occur only when there is interference between levels of opposite parity.

mis-alignment of the axis of rotation of the counters with respect to the target. Therefore, all the data at angles greater than 90^{o} were reduced by 2%, which was the average value of the asymmetry about 90^{o} for all of the angular distributions in this reaction.

The background radiation was measured at each of the energies in question and was found to be negligible for the coincidence counters. The background for the monitor counter was about the same as the statistical error (1/2 - 1%) from the number of counts. Since the usual variations in bombarding time for a given amount of charge were less than 15%, the background was essentially constant and therefore no correction was required.

Other possible sources of error are in counting losses due to Geiger counter dead-time and accidental coincidences due to the finite resolving time of the coincidence circuit. The first varied from about 2 to 4% but is rather uncertain because of the difficulties in measuring counter dead times. The latter varied from 0.5 to 1.5% at different energies. However, in the course of the angular distribution measurements at any given energy the beam current (and therefore these errors) usually varied less than 15%, hence the correction would be nearly the same for all the data in one distribution unless there were a large anisotropy. At the only resonance where this occurred the counting rate was lowered so as to minimize these errors. For the reasons outlined above no corrections were applied for dead-time losses or accidental coincidence errors. The final justification for neglecting these corrections is that the effect of such errors on the angular distributions measured is considerably less than the error due to statistical fluctuations in the counting rate.

The results of the angular distribution measurements are plotted in Figures 3 - 9 as a function of $\cos^{2}\theta$, the errors indicated on each point being the statistical standard deviation calculated from the number of counts. Any terms in $\cos^{4}\theta$ in the angular distribution would produce a parabola when plotted versus $\cos^{2}\theta$; hence we see that the data are best fitted by a curve of the form

+ a $\cos^2\theta$. The coefficients a were calculated by the method of least squares, hile the errors in a indicated are the standard deviations which can be com- uted from the goodness of fit of the data to the calculated curve.

A very surprising result was the fact that the front counter gave early the same angular distribution as the front and back counters in coincidence. ne would have expected that radiation scattered from the shielding surrounding he detectors and target chamber would considerably reduce any asymmetry in the eadings of a single counter. In only two cases are the coefficients a signifi- antly different for the angular distribution as measured by a single counter and y coincidence counters, and in each of these cases the single counter gives a maller asymmetry. A possible explanation for this is the effect of annihilation adiation from nuclear pairs, which would make a smaller for the front counter.

The results of the angular distribution measurements are collected in able I, which also gives the values of a corrected for the counter resolution.

TABLE I

Angular Distributions of γ-rays from $F^{19}(p,\alpha\gamma)O^{16}$ $I(\theta) = 1 + a\cos^2\theta$

E_R(kev)	a (observed)	a (corrected)*
873.5	0.103 ± .006	0.107
935	- 0.0028 ± .0053	- 0.0029
1290	0.644 ± .017	0.668
1355	0.224 ± .016	0.233
1373	- 0.214 ± .013	- 0.222
1381	- 0.070 ± .015	- 0.073
1405	0.138 ± .011	0.143

* Counter resolution: $2\alpha = 14.5^\circ$

$$\frac{b}{\rho} = \tan 16.5^\circ$$

In order to compare these results with the theory it is necessary to transform them to a frame of reference in which the excited O^{16} nucleus is at rest. This involves a correction that arises from the transformation of coordinates plus a correction for the change in detector efficiency caused by the Doppler effect. These effects are discussed by Devons and Hine[3], who show that they lead to terms in $\frac{v}{c}\cos\theta$, where v is the velocity of the recoiling nucleus and c the velocity of light. In this reaction the motion due to the recoil of the Ne^{20} compound state is so small as to have a completely negligible effect on the angular distribution. The recoil of the O^{16*} nucleus is considerably larger, but unless the angular distribution of α-particles is quite asymmetric this will also have a negligible effect. In fact, even if all the α-particles were emitted in the forward direction the correction term for this motion would only be about $0.02\cos\theta$. One other effect will tend to counteract this. The length of time for the recoiling O^{16*} nucleus to slow down in the target is of the order of 10^{-13} sec, which is also of the order of magnitude of the half life for the γ-ray transition. Thus, even in the most unfavorable case we feel that the errors introduced by omitting these corrections for recoil motion will be unimportant.

In the region from 1250 to 1400 kev proton energy the angular distribution of the γ-rays changes markedly. This is shown in Figure 10, where we have plotted the number of coincidence counts at 0° and 90° as a function of energy, as well as the coefficient a, which is equal to $I(0^\circ)/I(90^\circ)$ minus one. It is interesting to note that from 1350 to 1400 kev the maxima and minima in a do not occur at the maxima and minima in the yield curves as one might expect. At first sight this suggests an interference effect. However, the interpretation is complicated by the fact that three different γ-rays are present here.

(2) $C^{12}(p,\gamma)N^{13}$

The investigation of the γ-rays from the resonance in this reaction at 1696 kev was undertaken in the hope that it would help in explaining the anomalies that appear in the elastic scattering of protons here[13]. The only previous work on this reaction was by Van Patter[14], who obtained a resonance energy of 1697 ± 12 kev and a half width of 74 ± 9 kev.

In order to obtain a reasonable counting rate it was necessary to move

the counters up so that the front counter was only 1 1/2" from the target. Another, identical coincidence counter framework was also constructed in order to speed up the process of taking data. Both coincidence counter arrangements had .030" of aluminum absorber between the counters. This was sufficient to eliminate coincidence counts from the annihilation radiation present. The converter was 1/8" of aluminum immediately in front of the front counter. In addition it was found advantageous to use 1/8" of lead in front of this to eliminate soft radiation from the target backing.

In preliminary investigations a number of excitation curves were run on this resonance and the strong one at 1754 kev in $C^{13}(p,\gamma)N^{14}$. From the shape of the yield for the latter reaction, it is apparent that the target was non-uniform. A typical curve is shown in Figure 11. Because of its very small natural half-width ($\Gamma \approx 2$ kev) the shape of the yield curve for the $C^{13}(p,\gamma)N^{14}$ resonance is determined essentially by the target. For this particular target one can see that the target varies approximately linearly from a thickness of $1/4\,\Gamma$ to $3/4\,\Gamma$, where Γ is the natural width (= 68 kev) of the $C^{12}(p,\gamma)N^{13}$ resonance at 1696 kev. The other target used varied in thickness from $1/2\,\Gamma$ to Γ. In the Appendix a formula is derived for the effect of such targets on the shape of an excitation curve. It is shown there that if $\bar{\xi}$ is the average thickness of the target, then the energy at the peak of the curve is $E_R + \frac{1}{2}\,\bar{\xi}$ and the width from the low energy half intensity point to the peak is $\frac{1}{2}\sqrt{\Gamma^2 + \bar{\xi}^2}$. Thus it was possible to use these curves to infer the resonance energy and half width. The mean values obtained from eight runs are $E_R = 1696 \pm 5$ kev (based on a value of 1754 ± 3 kev for the $C^{13}(p,\gamma)N^{14}$ resonance from unpublished work of Perry and Day) and $\Gamma = 69 \pm 5$ kev. The errors quoted are twice the standard deviations of the mean in order to allow for hidden errors.

Two yield curves were also run with thick targets, which agreed rather

well with the preceding results. However, here it is necessary to make a correction for the fact that the $C^{12}(p,\gamma)N^{13}$ yield has not risen to its full maximum at the energy at which the $C^{13}(p,\gamma)N^{14}$ step occurs. Taking this into account by using the previous data, we obtain from the two thick target curves the average values E_R = 1697 kev and Γ = 68 kev. The ratio of the thick target step of the $C^{12}(p,\gamma)N^{13}$ resonance at 1696 kev to that of the $C^{13}(p,\gamma)N^{14}$ resonance at 1754 kev was 2.8 $\pm$ .3 with the counter arrangement used.

The angular distribution for this resonance in $C^{12}(p,\gamma)N^{13}$ was measured with a target of 54 kev average thickness at three energies: 1682, 1723 and 1749 kev. The first energy was approximately at the low energy half-maximum, the second was at the peak; and the third was as close to the $C^{13}(p,\gamma)N^{14}$ resonance at 1754 kev as we could get without interference from it. Figure 12 shows the averages of two complete measurements at each of the energies, corrected for the background radiation from the target backing. During preliminary measurements the target backing bowed out from its normal position because of the heat generated by the proton bombardment. A correction of the order of 3% was made for this in the data appearing in Figure 12. No correction was made for dead-time losses or accidental coincidences since the error due to neglecting these was many times smaller than the statistical error. It can be seen that each of the angular distributions is best fitted by a curve of the form $1 + \underline{a} \cos^2\theta$. The coefficients $\underline{a}$ listed in Table II were calculated by the method of

TABLE II

Angular Distribution of γ-rays from $C^{12}(p,\gamma)N^{13}$

$$I(\theta) = 1 + a \cos^2\theta$$

E_p (kev)	a (observed)	a (corrected)*
1682	- 0.394 $\pm$ .051	- 0.473
1723	- 0.474 $\pm$ .017	- 0.568
1749	- 0.516 $\pm$ .016	- 0.618

* Counter resolution: $2\alpha = 36^\circ$

$$\frac{b}{\rho} = \tan 37.5^\circ$$

least squares; the errors given are the standard deviations calculated from the goodness of fit of the data to the calculated curve. Table II also gives the values of $\underline{a}$ corrected for the detector resolution. It will be observed that $\underline{a}$ varies approximately linearly as we pass through the resonance. It is believed that this change is significant. Its interpretation will be discussed in the following section.

At one time the possibility was suggested that the γ-rays from this level might cascade to the ground state by means of an intermediate level. To check this point the range of the secondary electrons was measured by placing various amounts of aluminum absorber between the coincidence counters. Figure 13 shows the results of an absorption measurement at 1723 kev proton energy compared with the absorption of secondaries from ThC". Both curves have been corrected for background counts and accidental coincidences. Using Schardt's charts[15], which were prepared for a similar arrangement, we find that the γ-ray energy is $3.5 \pm .1$ Mev and that there is no evidence of lower energy radiation.

(3) $C^{13}(p,\gamma)N^{14}$

Having observed the resonance in this reaction at 1754 kev so often in our work with natural carbon targets, it was only natural to try to measure its angular distribution. For this purpose a target was made by mixing some thin shellac with C^{13} enriched lamp black and spreading the mixture out thin on a tantalum foil. The detector arrangement was identical with that of the previous experiment, with the exception that 1/4" of aluminum absorber was placed between the coincidence counters. This change was made in order that the measured distribution be essentially that of the 9.2 Mev transition to the ground state.

Figure 14 shows the results of the angular distribution, as well as an excitation curve taken with .150 inches of aluminum absorber. The slow drop in

intensity on the high energy side of the resonance is caused by the non-uniformity of the target. The angular distribution was measured at the energy indicated by the arrow (1.77 Mev) and also below the sharp step (1.67 Mev). The points plotted as a function of $\cos^2\theta$ are the difference between the values thus obtained and therefore are representative of the radiation from this resonance alone. Again, the corrections for dead-time losses and accidental coincidences were negligible and hence were not made. It can be seen that the data fit a curve of the form $1 + \underline{a} \cos^2\theta$ very well. A least squares calculation gives $\underline{a} = -0.399 \pm .012$. The coefficient corrected for counter resolution is $\underline{a} = -0.479$.

IV. INTERPRETATION OF THE RESULTS

The question of the angular distribution of γ-rays from a nucleus has been treated by a number of authors[16 - 20]. Heitler[16] has derived a general expression in closed form for the vector potential of any magnetic or electric multipole and has shown that the radiation field carries angular momentum. His formulas are more conveniently available in Ling and Falkoff's paper[17]. The physical concepts involved in applying these to the calculation of the angular variation of γ-ray intensities in a nuclear process have usually been concealed by a cloud of fearsome symbols and complicated quantum mechanics. The paper of Devons and Hine[18] is a welcome relief, and even more understandable are the Cambridge notes of French[19]. Chao[20] also has an interesting discussion of the principles involved, although not so complete as the above.

The essential angular information is contained in the field distribution of the multipole; that is, this is the only point in the calculations at which an angle enters in. The rest of the calculations deal only with the transformation properties of angular momentum vectors. Instead of producing a general formula let us introduce a few simple examples to illustrate the principles involved. The following notation will be employed:

J = Angular momentum of compound nucleus.

M = Component of J along axis of quantization (usually the direction of the beam).

j = Angular momentum of a given spin state of the proton and target nucleus.

m = Component of j along axis of quantization.

ℓ = Relative orbital angular momentum of proton and target nucleus.

L = Multipole order = angular momentum of multipole.

m' = Component of L along axis of quantization.

All angular momenta are in units of $\hbar$.

(1) Consider the case of a radioactive nucleus undergoing a γ-ray transition from an excited state with J = 3/2 to the ground state of J = 1/2 and suppose that the parities of the two states are opposite. The conservation of angular momentum and parity shows us that the radiation must be electric dipole or magnetic quadrupole. However, in general the intensity of magnetic quadrupole radiation will be very much lower than that of electric dipole, hence we consider only the latter. We now find the probability that each sub-state (designated by M) of the excited state decays in a given way. These probabilities are the squares of the transformation coefficients for angular momenta, which are tabulated in Cohen's thesis[21]. Multiplying the intensity distribution for a given mode of decay by the probability of that mode and summing, we obtain the intensity distribution for the decay of that sub-state. Summing then over the various sub-states weighted according to their statistical probability gives us the angular distribution to be compared with an experiment.

From the tables in Cohen's thesis we find that the sub-states with $M = \pm 3/2$ can decay by L = 1 (dipole) only if m' = 1. Thus if F_J^M is the intensity distribution from the sub-state designated by J, M we obtain from

Ling and Falkoff's paper

$$F^{\pm 3/2}_{3/2} = \frac{3}{2}(1 + \cos^2\theta)$$

The states with $M = \pm 1/2$ decay 2/3 of the time by $L = 1$, $m' = 0$ and 1/3 of the time by $L = 1$, $m' = \pm 1$. Thus

$$F^{\pm 1/2}_{3/2} = \frac{2}{3} \cdot 3(1 - \cos^2\theta) + \frac{1}{3} \cdot \frac{3}{2}(1 + \cos^2\theta)$$

Since the a priori probabilities of the sub-states M are equal for a radioactive nucleus, we obtain for the angular distribution

$$F_{3/2} = \sum F^{M}_{3/2} = 2 \cdot 3/2\,(1 + \cos^2\theta) + 2 \cdot 2\,(1 - \cos^2\theta) + 2 \cdot 1/2\,(1 + \cos^2\theta) .$$

$$= 8$$

As one would have expected this is independent of the angle of observation.

(2) Let us now calculate the angular distribution of the γ-rays produced in the reaction $C^{12}(p,\gamma)N^{13}$ when the compound nucleus has $J = 3/2$ and even parity. Since the ground state of N^{13} presumably has spin 1/2 and odd parity, the situation here differs from the first case only in that the various sub-states M no longer have equal statistical weights. Thus the only new part of the problem is to determine these.

Because of the fact that C^{12} and the proton have even intrinsic parity, the parity of the compound nucleus will be that of the relative orbital motion of the proton and C^{12}. Hence, only waves of even angular momentum can be involved, and of these only d-wave can produce a state of $J = 3/2$ (since $J = \pm 1/2$). From the tables of transformation coefficients we find that the probabilities for the formation of the $M = \pm 3/2$ sub-states are zero, while the probabilities for the $M = \pm 1/2$ sub-states are equal. Therefore,

$$F_{3/2} = F^{-1/2}_{3/2} + F^{1/2}_{3/2} = 4(1 - \cos^2\theta) + 1(1 + \cos^2\theta)$$

$$= 5(1 - 3/5\,\cos^2\theta)$$

Other cases will be essentially the same but the actual details may be more involved. If two or more spin states of the initial configuration (designated by j, m) can combine with the orbital angular momentum to give the same state of the compound nucleus, the probability for the formation of the latter may depend on nuclear factors involving the spin in some unknown way. This case can be taken into account by means of arbitrary constants. Similarly, different waves of orbital angular momentum may be involved and will of course depend on the barrier penetration as well as possibly unknown nuclear factors. Another question that arises is whether one should add amplitudes or intensities. Of course, if different energy γ-rays are present they do not interfere. However, for a given γ-ray energy, in general one adds amplitudes only when different angular momenta of the incoming beam are involved or for different multipole orders of the radiation. One always adds intensities whenever different sub-states of the initial or final state are involved.

Thus we see that the calculation of γ-ray angular distributions is essentially equivalent to the determination of the radiation pattern for a number of different antennas oriented in various directions. The realization of this fact enables one to extend these results to the calculation of the correlation of a particle and γ-ray emitted in sequence or to the correlation between two successive γ-rays. However, the details will not be considered here.

(1) $F^{19}(p,\alpha\gamma)O^{16}$

The interpretation of the angular distributions in the fluorine reaction has been discussed in detail by Chao[20]. From the observed angular distribution of the long-range α-particles and of the α-particles that go to the pair level in O^{16}, he concludes that F^{19} has even parity. Arnold's experiment on the $\alpha - \gamma$ correlation at the 340 kev resonance[5] clearly demonstrates that the 6.14 Mev level in O^{16} has $J = 3$ and odd parity. Assuming that the observed

γ-rays are from the 6.14 Mev level Chao then concludes that the excited states of Ne^{20} involved in the various resonances have spin and parity as shown in Table III. The orbital angular momentum of the proton is also shown under ℓ_p.

TABLE III

Angular Momenta of Ne^{20} Levels Involved in the Reaction $F^{19}(p,\alpha\gamma)O^{16}$

Resonance	$J(Ne^{20})$	ℓ_p
340	1+	0
598	2-	1
669	1+	0
874	1+ or 2^-	0,2 or 1
935	1+	0
1290	3+	2
1355	3+	2
1381	1+	0,2

It remains to explain the anomalous behavior of the angular distribution in the region from 1250 to 1400 kev proton energy. Here the relative proportions of the three γ-ray components change rapidly and become of comparable intensity at 1355 kev. Accordingly it is felt that an analysis is not possible on the basis of the present data. This problem can be better attacked by measuring the angular correlation between the various α-particle groups and the γ-ray following them. Because of the lower energy of the α-particles (1 - 2 Mev), it should be possible to resolve them with a scintillation counter.

(2) $C^{12}(p,\gamma)N^{13}$

This reaction at 1696 kev provides possibly as favorable a case as can be found for an unambiguous interpretation of the experimental results. The reason is that the C^{12} target nucleus has spin 0 and therefore the spin of the

compound nucleus is $J = \ell \pm 1/2$. In addition, the half width is so great that it could not reasonably be produced by any component of the proton beam with $\ell > 2$.* Thus we can limit ourselves to states of the compound nucleus with $J \leq 5/2$. The angular distributions to be expected for the various possibilities are given in Table IV. The assumption is made here that the ground state of N^{13} has spin 1/2 and odd parity. This is what would be expected on the basis of the shell model. The assignment of $J = 1/2$ to the compound nucleus is clearly ruled out by the large observed asymmetry. Spin 5/2 also is unreasonable, since any combination of r and that would give a coefficient of about - 0.6 for the $\cos^2\theta$ term would also give a comparable coefficient for the $\cos^4\theta$ term. A coefficient this large would certainly have been detected in the measurements. We are thus led to the conclusion that the correct spin is 3/2; however, the angular distribution at only one energy cannot settle the problem of the parity.

The results of the angular distributions at three energies show a variation with energy that is approximately linear. This variation cannot be accounted for by the radiation from a single level, hence we are forced to consider the possibility that two overlapping levels are involved here. One would expect terms in $\cos\theta$ if the levels were of opposite parity. The absence of such terms indicates the contrary, but we must not lean too strongly on this argument at first for we would also expect the coefficient of the $\cos\theta$ term to vanish near the resonance and it might have been too small to be observed at the other energies.

In attempting to decide on the character of the levels involved, calculations of the angular distributions as a function of energy have been made for the following combinations:

(a) Resonant $J = 3/2$, even, and non-resonant $J = 1/2$, even

---

* For d-wave ($\ell = 2$) the reduced width is 2 Mev.

TABLE IV

Angular Distributions in the Reaction $C^{12}(p,\gamma)N^{13}$

For the Various Possible Spins and Parities of the Compound Nucleus

$J(N^{13*})$	Radiation	$I(\theta)$
1/2, even	electric dipole	isotropic
1/2, odd	magnetic dipole	isotropic
3/2, even	electric dipole	$1 - 3/5 \cos^2\theta$
3/2, odd	magnetic dipole and electric quadrupole	$1 - \dfrac{3r^2 - 6\sqrt{3}r\cos\eta - 3}{5r^2 - 2\sqrt{3}r\cos\eta + 3}\cos^2\theta$
		$1 + \cos^2\theta$ for $r = 0$
		$1 - 3/5\cos^2\theta$ for $r = \infty$
5/2, even	magnetic quadrupole and electric octupole	$1 + 6 \cdot \dfrac{4r^2 + 6\sqrt{2}r\cos\eta + 1}{4r^2 - 2\sqrt{2}r\cos\eta + 5}\cos^2\theta$
		$- 5 \cdot \dfrac{4r^2 + 10\sqrt{2}r\cos\eta - 1}{4r^2 - 2\sqrt{2}r\cos\eta + 5}\cos^4\theta$
		$1 + 6/5\cos^2\theta + \cos^4\theta$ for $r = 0$
		$1 + 6\cos^2\theta - 5\cos^4\theta$ for $r = \infty$

r = ratio of amplitude of magnetic radiation to electric radiation.

η = relative phase of magnetic and electric radiation.

(b) Resonant J = 3/2, odd, and non-resonant
J = 1/2, odd

(c) Resonant J = 3/2, odd, and non-resonant
J = 1/2, even

(d) J = 3/2, even and J = 5/2, even, resonant at different energies.

Other combinations might also have been considered, but these seemed the most reasonable. If we neglect the possible electric quadrupole radiation from the J = 3/2 level in case (b), both (a) and (b) give the same results. Case (d) gives a coefficient of the $\cos^2\theta$ term that is quadratic in energy, as well as a term in $\cos^4\theta$. However, with six undetermined constants the formula could probably fit nearly anything. Perhaps the simplest and most easily tested assumption is that one of the levels is the tail of the one at 456 kev, which would be essentially constant over the range of energies considered here. This level almost certainly has J = 1/2, even; therefore, we examine more carefully the formulas for (a) and (c). These are:

(a)
$$I(\theta) = 1 - \frac{3/4\, r^2 + \frac{\sqrt{3}}{2}\, r\,(x\cos\delta - \sin\delta)}{x^2 + 1 + 5/4\, r^2 + \frac{r}{\sqrt{2}}(x\cos\delta - \sin\delta)}\cos^2\theta$$

where $x = 2/\Gamma\ (E - E_r)$

$r = \dfrac{\text{amplitude of electric dipole from J = 3/2, even}}{\text{amplitude of electric dipole from J = 1/2, even}}$

δ = relative phase of the two γ-rays.

(c)
$$I(\theta) = 1 - \frac{\sqrt{6}r_2\ x\sin(\delta-\eta) + \cos(\delta-\eta) + \sqrt{2}r_1[x\sin\delta + \cos\delta]}{x^2 + 1 + 5/4\, r_1^2 + 3/4\, r_2^2 - \frac{\sqrt{3}}{2}\, r_1 r_2\cos\eta}\cos\theta$$
$$- \frac{3/4 r_1^2 - 3/4 r_2^2 - \frac{3\sqrt{3}}{2}\, r_1 r_2\cos\eta}{x^2 + 1 + 5/4\, r_1^2 + 3/4\, r_2^2 - \frac{\sqrt{3}}{2}\, r_1 r_2\cos\eta}\cos^2\theta$$

where $r_1 = \dfrac{\text{amplitude of magnetic dipole from J = 3/2, odd}}{\text{amplitude of electric dipole from J = 1/2, even}}$

$r_2 = \dfrac{\text{amplitude of electric quadrupole from J = 3/2, odd}}{\text{amplitude of electric dipole from j = 1/2, even}}$

δ = phase of electric dipole relative to magnetic dipole

η = phase of electric quadrupole relative to magnetic dipole

Case (c) does not seem to fit the observed data: it has a term in cos θ and the coefficient of $\cos^2\theta$ varies only slightly with energy and not linearly. The coefficient of $\cos^2\theta$ in case (a), however, has the required linear variation. To obtain a numerical check we have extrapolated the cross section of the 456 kev resonance to 1696 kev using the Breit-Wigner formula

$$\sigma \sim \frac{1}{E} \frac{\Gamma_\gamma \Gamma_p}{(E - E_r)^2 + (\Gamma/2)^2}$$

Γ_γ varies as the third power of the γ-ray energy for electric dipole radiation, while the energy variation of Γ_p was obtained from the curves of Christy and Latter[22]. Using Γ = 35 kev we obtain

$$\sigma/\sigma_r = .0046$$

Van Patter[14] has found that the ratio of the thick target yields for the 1696 kev and 456 kev resonances is 1.3. Using this data we find that

$$r = \sqrt{\frac{\sigma_{1696}(1696)}{\sigma_{456}(1696)}} = \sqrt{55.3} = 7.4$$

If the calculation were done more rigorously the value of r might be greater by perhaps a factor of $\sqrt{2}$. Therefore in comparing the formulas for the angular distributions with the experimental results we take r = 10. Assuming the expected distribution to vary linearly with energy a calculation shows that the energies at which the results are to be compared are $E_r - \Gamma/2$, E_r, and $E_r + .59\ \Gamma/2$. If we take $\delta = 0$ we obtain the results shown in Table V.

TABLE V

Energy	$\underline{a}$ (Experimental)	$\underline{a}$ (Calculated)
$E_r - \Gamma/2$	- 0.473	- 0.448
E_r	- 0.568	- 0.595
$E_r + .59\ \Gamma/2$	- 0.618	- 0.670

We see from the table that the hypothesis that the level in N^{13} at 1696 kev has J = 3/2 and even parity explains the results of this experiment quite well.

It must be mentioned that the above interpretation does not fit all the experiments in which this level takes part. From the energy shift of this level relative to the corresponding one in the mirror nucleus C^{13}, R. G. Thomas has concluded that it must have J = 3/2 and odd parity[23]. To further complicate the issue, the elastic scattering of protons at this energy[13] cannot be adequately explained by either assignment. The latter experiment would seem to require a doublet. If the two levels of the doublet were $^2d_{3/2}$ and $^2d_{5/2}$, then the radiation from the $^2d_{5/2}$ state could be expected to be much less intense than that from the other and might not be observed. Thus, it is not possible at this time to make a final statement on the nature of this level. A measurement of the angular distribution of the elastically scattered protons at various energies would probably best reveal the information we need.

$C^{13}(p,\gamma)N^{14}$

Devons and Hine[18] have calculated the angular distributions to be expected for various levels of the N^{14} nucleus. However, there is considerable ambiguity here, since the calculated formulas contain several undetermined constants, which allow the coefficient a to take on a range of values. Consequently we can only say that the assignment of J = 1, even, J = 2, even, and J = 2, odd, could fit the observed results. The strength of the radiation at this resonance would suggest that it is electric dipole. If this is true, the level probably has J = 2, odd.

APPENDIX I

THE EFFECT OF NON-UNIFORM TARGETS ON RESONANCE REACTION YIELDS.

The Breit-Wigner formula for the energy dependence of the cross section of a reaction showing a resonance can be written, neglecting wave length and penetration factors as

$$\sigma = \frac{\Gamma^2}{4}\sigma_r \frac{1}{(E-E_r)^2 + \Gamma^2/4}$$

where E_r = resonance energy

Γ = width at half maximum

σ_r = cross section at resonance

The yield measured with a target of thickness ξ becomes

$$Y = \frac{\Gamma}{2\epsilon}\sigma_r \left\{ \tan^{-1}\frac{E-E_r}{\Gamma/2} - \tan^{-1}\frac{E-E_r-\xi}{\Gamma/2} \right\}$$

where ϵ = stopping cross section per disintegrable nucleus at the resonance energy.

Now assume that the target varies linearly from a thickness ξ_0 to $\xi_0 + a$. Then

$$Y = \frac{\Gamma}{2\epsilon}\sigma_r \int_0^1 \left\{ \tan^{-1}\frac{E-E_r}{\Gamma/2} - \tan^{-1}\frac{E-E_r-\xi_0-ax}{\Gamma/2} \right\} dx$$

$$= \frac{\Gamma}{2\epsilon}\sigma_r \left\{ \tan^{-1}\frac{E-E_r}{\Gamma/2} - \tan^{-1}\frac{E-E_r-\xi_0-a}{\Gamma/2} - \frac{E-E_r-a}{\Gamma/2} \times \right.$$

$$\left. \times \left[\tan^{-1}\frac{E-E_r-\xi_0}{\Gamma/2} - \tan^{-1}\frac{E-E_r-\xi_0-a}{\Gamma/2} \right] - \frac{1}{2}\frac{\Gamma/2}{a}\log\frac{1+\left(\frac{E-E_r-\xi_0-a}{\Gamma/2}\right)^2}{1+\left(\frac{E-E_r-\xi_0}{\Gamma/2}\right)^2} \right\}$$

This formula is too complicated to permit one to obtain a general solution for the energy at which the maximum yield occurs and the width of the excitation curve. Accordingly it was necessary to evaluate it numerically for the two cases of interest in the $C^{12}(p,\gamma)N^{13}$ reaction, namely

(1) $\xi_0 = \frac{1}{4}\Gamma$, $a = \frac{1}{2}\Gamma$

(2) $\xi_0 = \frac{1}{2}\Gamma$, $a = \frac{1}{2}\Gamma$

The results of the numerical evaluation are tabulated below

		Y_{max}	$\frac{1}{2} Y_{max}$ (low energy side)	Γ'
(1)	E	$E_r + 0.50 \frac{\Gamma}{2}$	$E_r - 0.64 \frac{\Gamma}{2}$	1.14Γ
(2)	E	$E_r + 0.75 \frac{\Gamma}{2}$	$E_r - 0.52 \frac{\Gamma}{2}$	1.27Γ

Γ' is twice the difference in energy between the point of maximum yield and the low energy half-maximum. For uniform targets equal in thickness to $\frac{1}{2}\Gamma$ and $3/4\,\Gamma$ the values of Γ' would be $1.12\,\Gamma$ and $1.25\,\Gamma$ respectively. Thus we see that the resonance energy and natural width can be obtained from the yield curves for non-uniform targets such as these by assuming that the targets have a uniform thickness equal to their average thickness.

APPENDIX II

CALCULATION OF THE EFFECTIVE PROTON ENERGY IN ANGULAR DISTRIBUTIONS FOR SEMI-THICK TARGETS.

Assume that we wish to measure an angular distribution of the form

$$I(\theta) = 1 + a \cos^2\theta$$

where $a = \alpha + \beta E$

If we let $E_p = E_r + x_1 \frac{\Gamma}{2}$ = bombarding energy

$\xi = x_1 \frac{\Gamma}{2} - x_2 \frac{\Gamma}{2}$ = target thickness

then the measured value of a for a resonance reaction will be

$$a = \frac{\int_{E_r + x_2 \Gamma/2}^{E_r + x_1 \Gamma/2} \frac{\alpha + \beta E}{(E - E_r)^2 + \Gamma^2/4} dE}{\int_{E_r + x_2 \Gamma/2}^{E_r + x_1 \Gamma/2} \frac{dE}{(E - E_r)^2 + \Gamma^2/4}}$$

$$= \alpha + \beta \left\{ E_r + \frac{1}{2} \frac{\log \frac{1 + x_1^2}{1 + x_2^2}}{\tan^{-1} x_1 - \tan^{-1} x_2} \cdot \frac{\Gamma}{2} \right\}$$

The effective proton energy is given by the expression in brackets.

REFERENCES

1. Burrows, Gibson, and Rotblatt, Phys. Rev. 80, 1095 (1950).
2. Krone, Hanna, and Inglis, Phys. Rev. 80, 603 (1950).
3. Devons and Hine, Proc. Roy. Soc. 199, 56 (1949).
4. Littauer, Proc. Phys. Soc. 63, 294 (1950).
5. W. R. Arnold, Phys. Rev. 80, 34 (1950).
6. Barnes, French, and Devons, Nature 166, 145 (1950).
7. R. M. Steffen, Phys. Rev. 80, 115 (1950).
8. Rose and Wilson, Phys. Rev. 78, 68 (1950).
9. Brady and Deutsch, Phys. Rev. 78, 558 (1950).
10. Beyster and Wiedenbeck, Phys. Rev. 79, 169 (1950).
11. Bennett, Bonner, Mandeville, and Watt, Phys. Rev. 70, 882 (1946).
12. Bernet, Herb, and Parkinson, Phys. Rev. 54, 398 (1938).
13. Goldhaber, Williamson, Jackson, and Laubenstein, Phys. Rev. 81, 310 (1951).
14. D. M. Van Patter, Phys. Rev. 76, 1264 (1949).
15. A. W. Schardt, PhD Thesis, California Institute of Technology (1951).
16. W. Heitler, Proc. Camb. Phil. Soc. 32, 112 (1936).
17. Ling and Falkoff, Phys. Rev. 76, 1639 (1949).
18. Devons and Hine, Proc. Roy. Soc. 199, 73 (1949).
19. A. P. French, Notes on Angular Distributions, Cambridge University (1950).
20. C. Y. Chao, Phys, Rev. 80, 1035 (1950).
21. E. R. Cohen, PhD Thesis, California Institute of Technology (1949).
22. Christy and Latter, Rev. Mod. Phys. 20, 185 (1948).
23. R. G. Thomas, Phys. Rev. (in press).

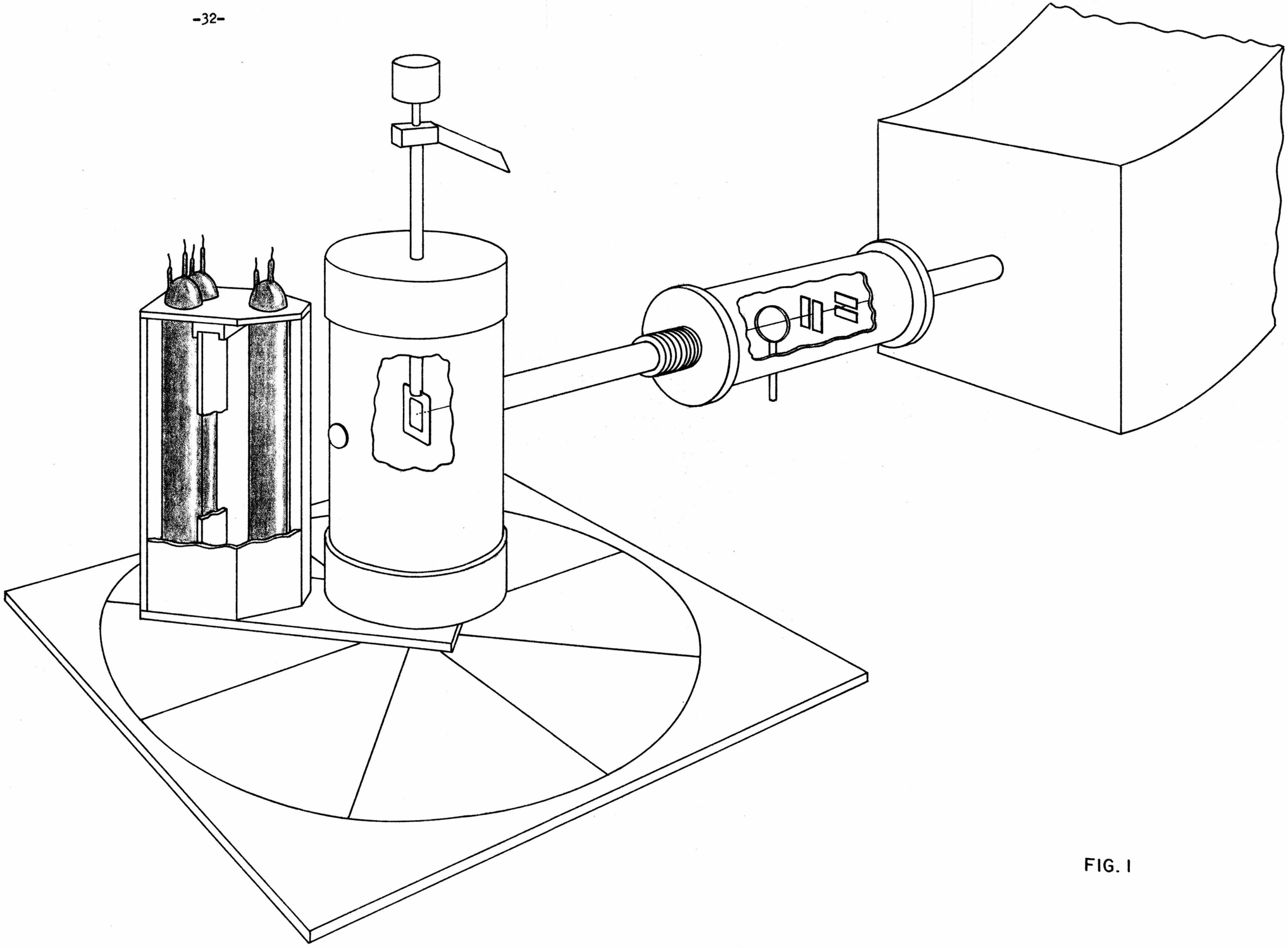

FIG. 1

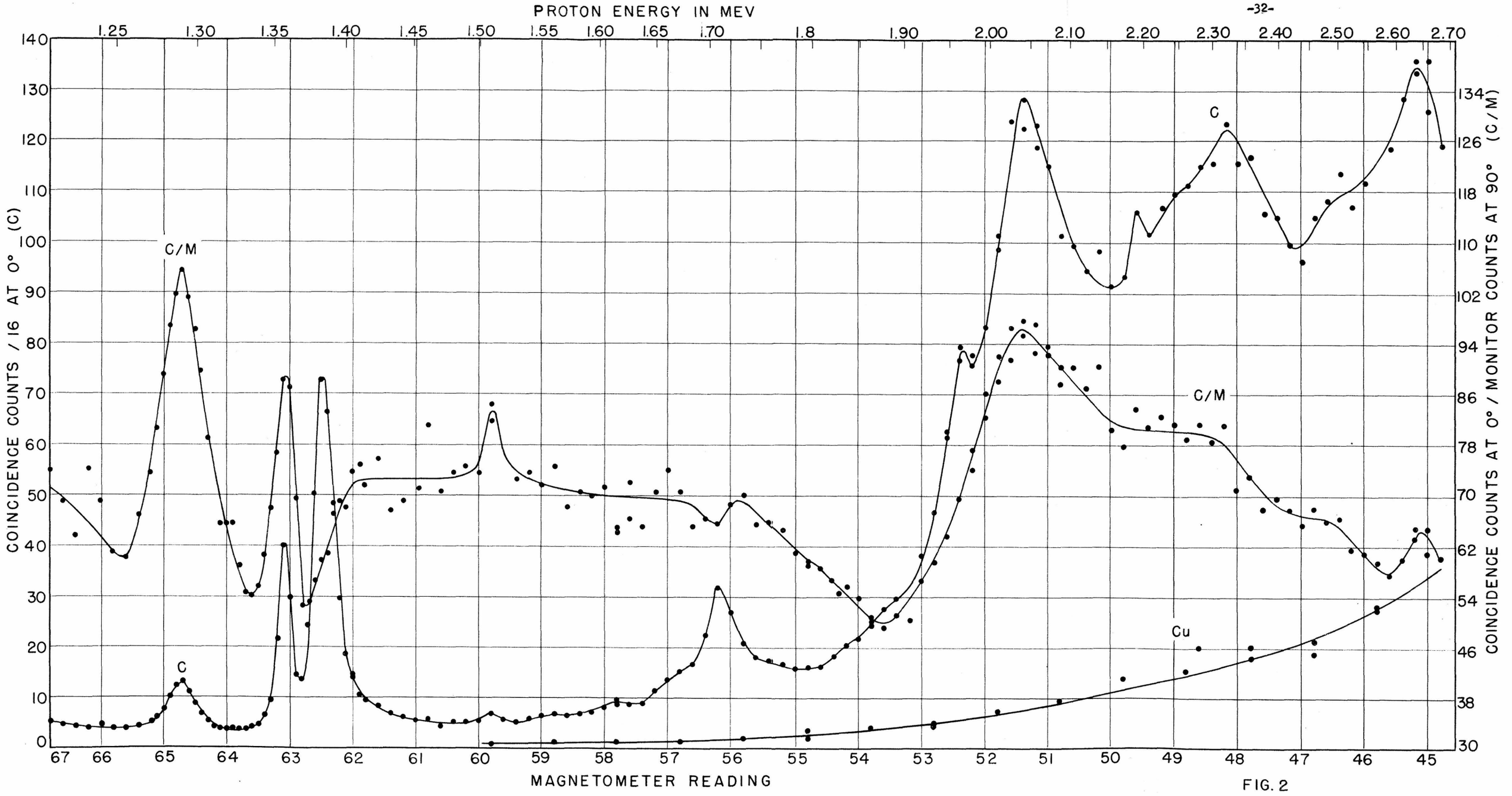
PROTON ENERGY IN MEV
1.25 1.30 1.35 1.40 1.45 1.50 1.55 1.60 1.65 1.70 1.8 1.90 2.00 2.10 2.20 2.30 2.40 2.50 2.60 2.70
COINCIDENCE COUNTS / 16 AT 0° (C)
0 10 20 30 40 50 60 70 80 90 100 110 120 130 140
COINCIDENCE COUNTS AT 0° / MONITOR COUNTS AT 90° (C/M)
30 38 46 54 62 70 78 86 94 102 110 118 126 134
C/M
C
C
C/M
Cu
67 66 65 64 63 62 61 60 59 58 57 56 55 54 53 52 51 50 49 48 47 46 45
MAGNETOMETER READING

FIG. 2

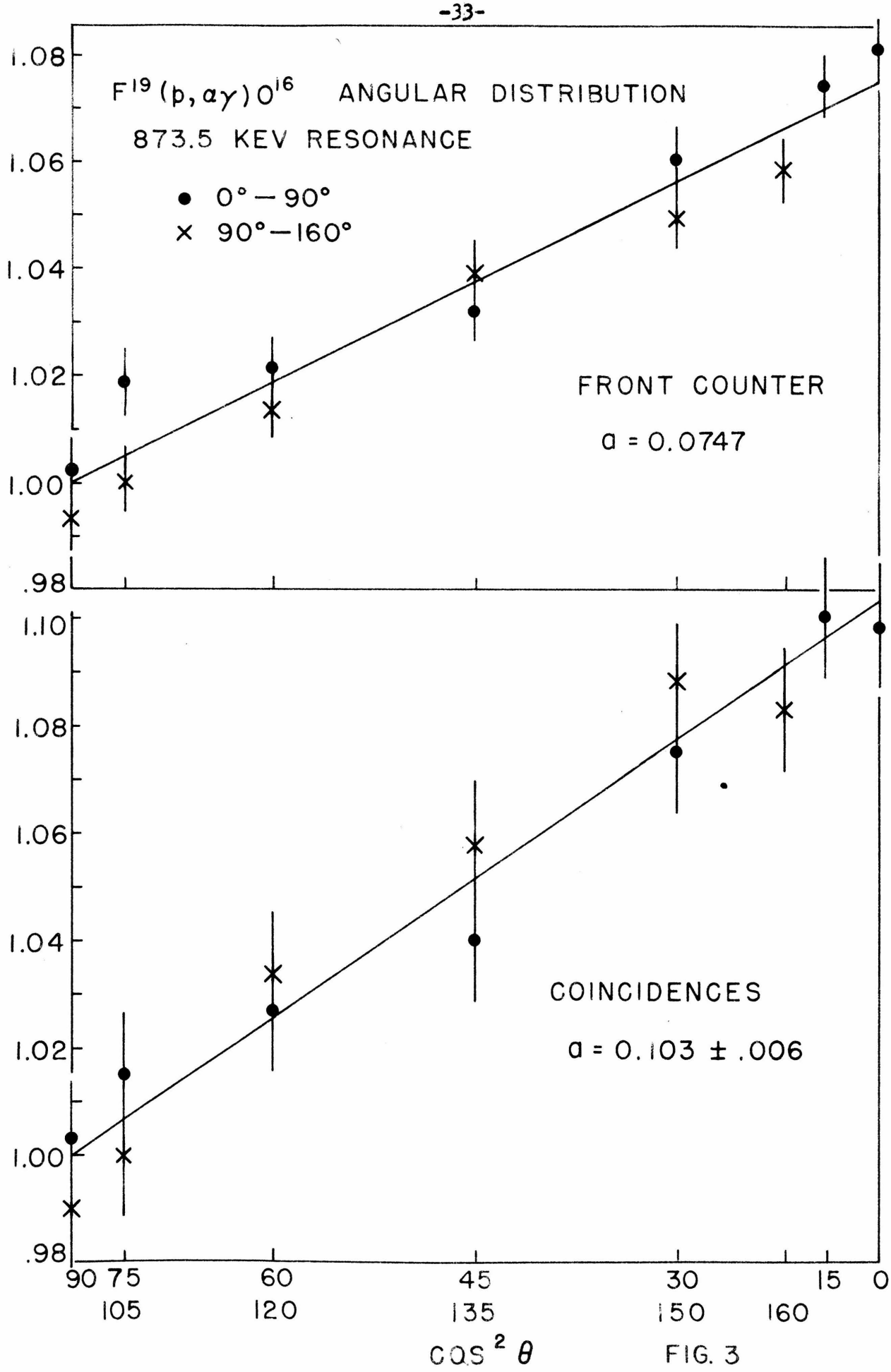
$F^{19}(p,\alpha\gamma)O^{16}$ ANGULAR DISTRIBUTION
873.5 KEV RESONANCE
● 0° — 90°
× 90° — 160°
FRONT COUNTER
a = 0.0747
COINCIDENCES
a = 0.103 ± .006
1.08
1.06
1.04
1.02
1.00
.98
1.10
1.08
1.06
1.04
1.02
1.00
.98
90 75 60 45 30 15 0
105 120 135 150 160
$\cos^2\theta$

FIG. 3

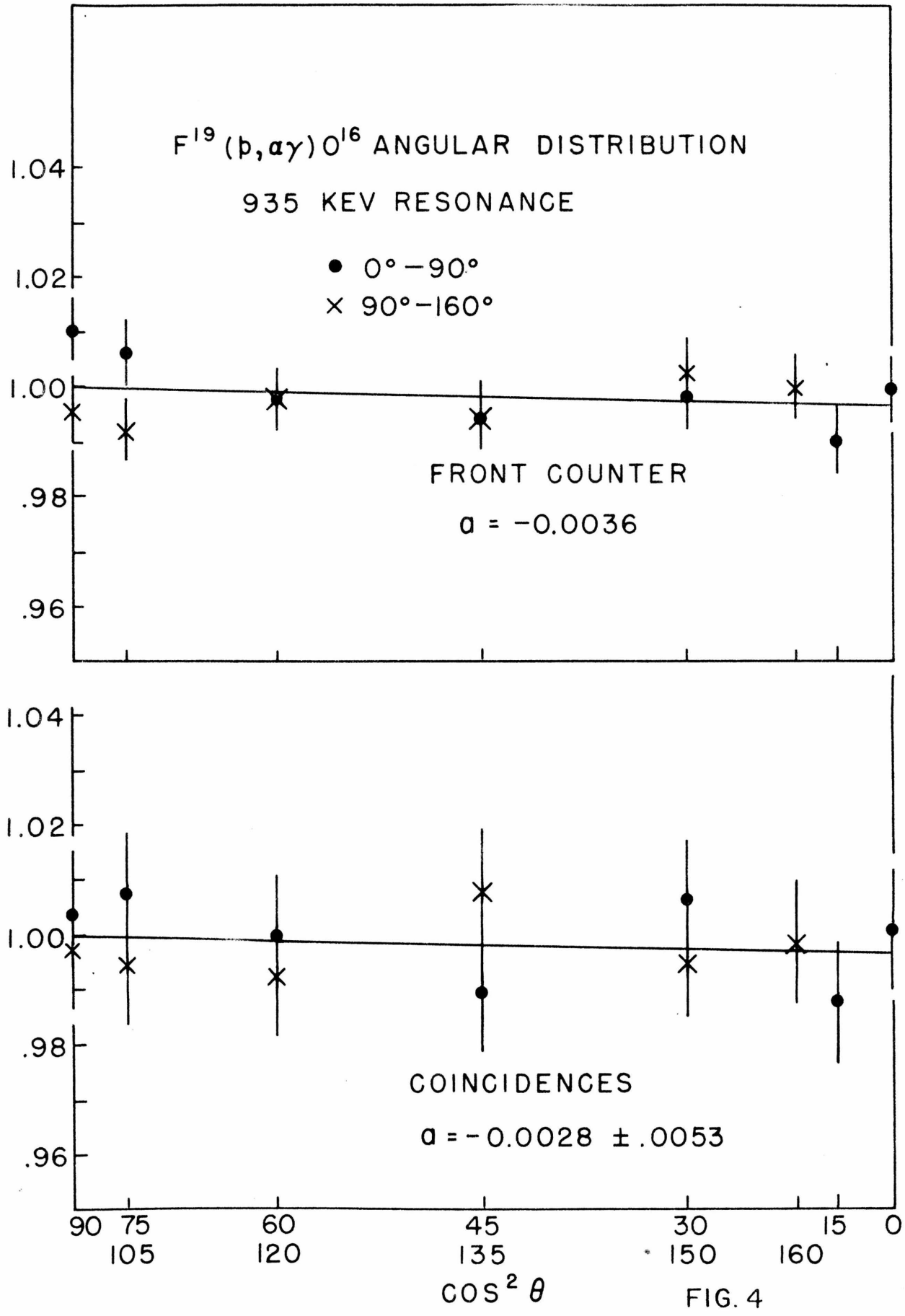
F19 (p, αγ) O16 ANGULAR DISTRIBUTION
935 KEV RESONANCE
● 0° – 90°
× 90° – 160°
1.04
1.02
1.00
.98
.96
FRONT COUNTER
a = −0.0036
1.04
1.02
1.00
.98
.96
COINCIDENCES
a = −0.0028 ± .0053
90 75 60 45 30 15 0
105 120 135 150 160
COS² θ

FIG. 4

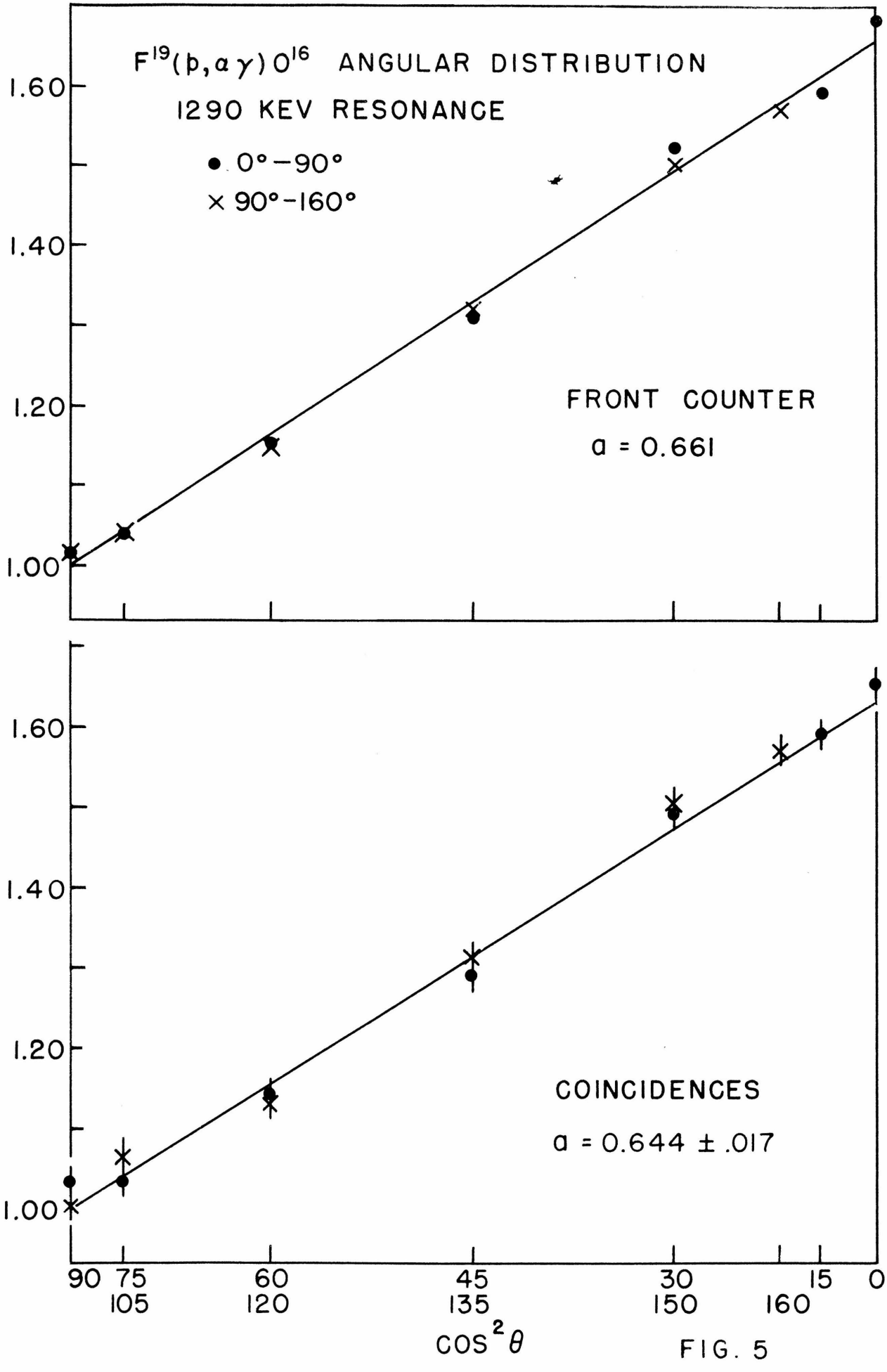
$F^{19}(p,\alpha\gamma)O^{16}$ ANGULAR DISTRIBUTION
1290 KEV RESONANCE
● 0°–90°
× 90°–160°
FRONT COUNTER
a = 0.661
COINCIDENCES
a = 0.644 ± .017
1.60
1.40
1.20
1.00
90 75 60 45 30 15 0
105 120 135 150 160
$\cos^2\theta$

FIG. 5

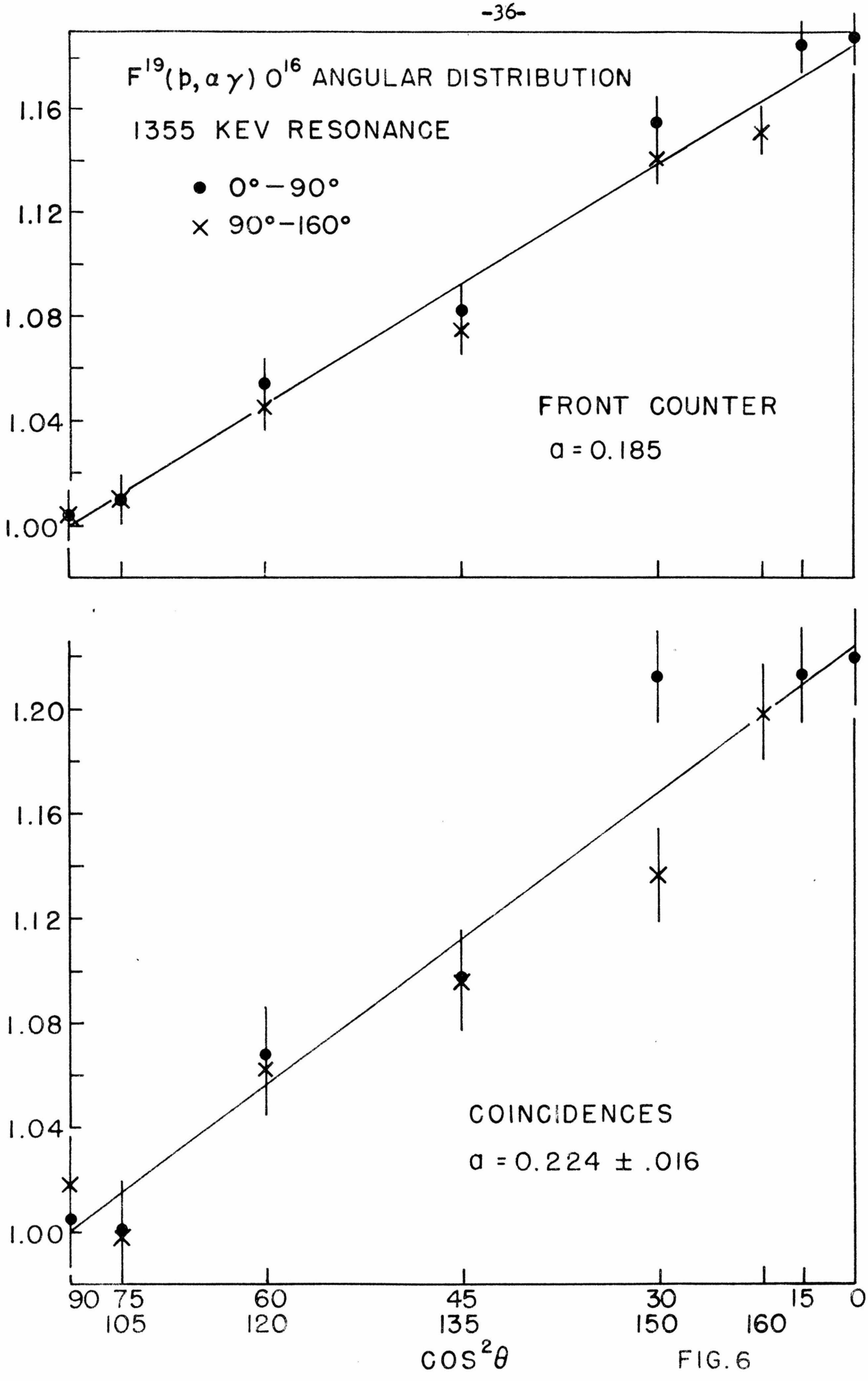
$F^{19}(p,\alpha\gamma)\,O^{16}$ ANGULAR DISTRIBUTION
1355 KEV RESONANCE
● 0°–90°
× 90°–160°
FRONT COUNTER
a = 0.185
COINCIDENCES
a = 0.224 ± .016
1.00
1.04
1.08
1.12
1.16
1.20
90 75 60 45 30 15 0
105 120 135 150 160
$\cos^2\theta$

FIG. 6

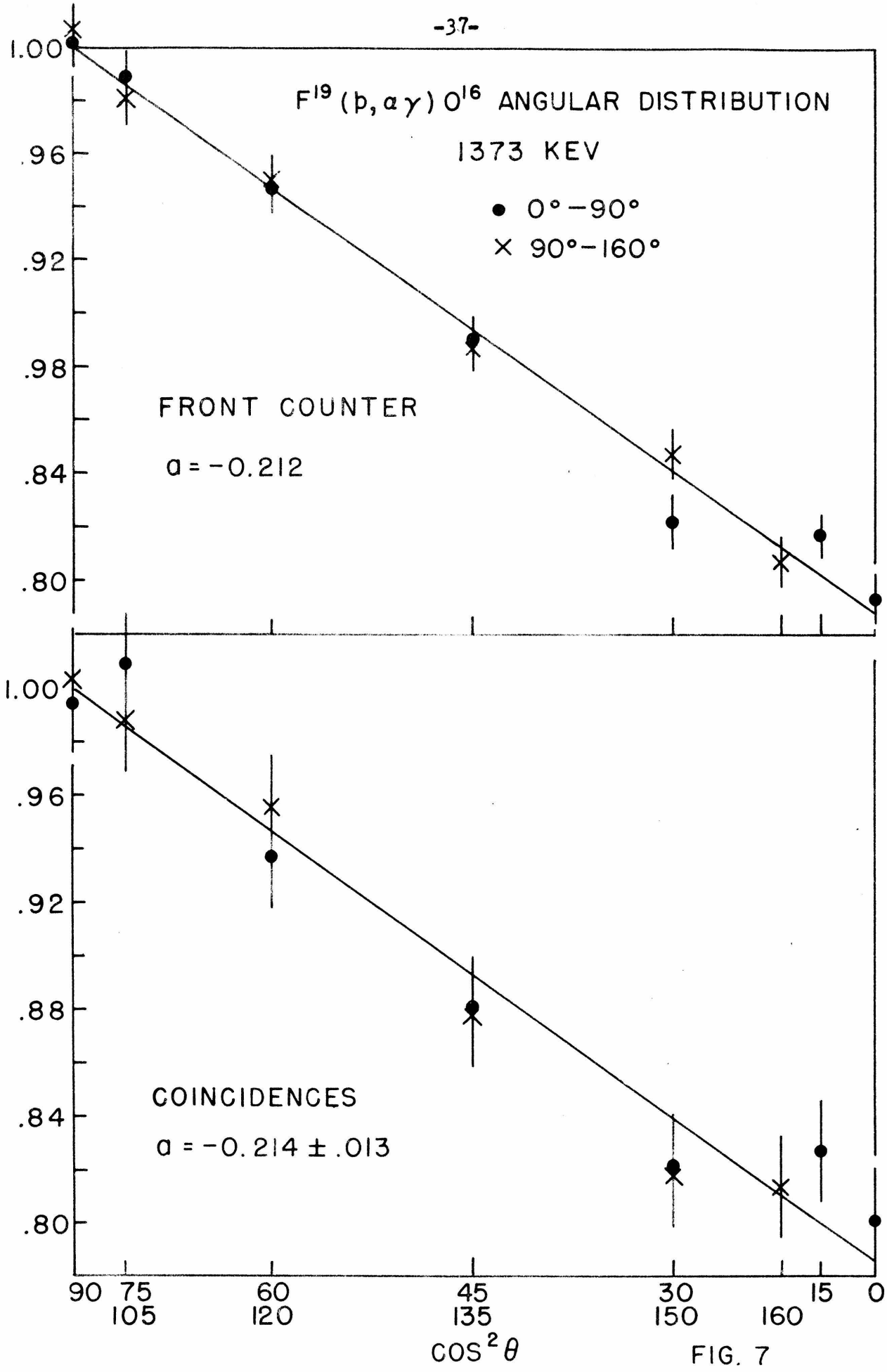
$F^{19}(p,\alpha\gamma)O^{16}$ ANGULAR DISTRIBUTION
1373 KEV
● 0°–90°
× 90°–160°
FRONT COUNTER
a = −0.212
COINCIDENCES
a = −0.214 ± .013
1.00
.96
.92
.98
.84
.88
.80
90 75 60 45 30 15 0
105 120 135 150 160
$\cos^2\theta$

FIG. 7

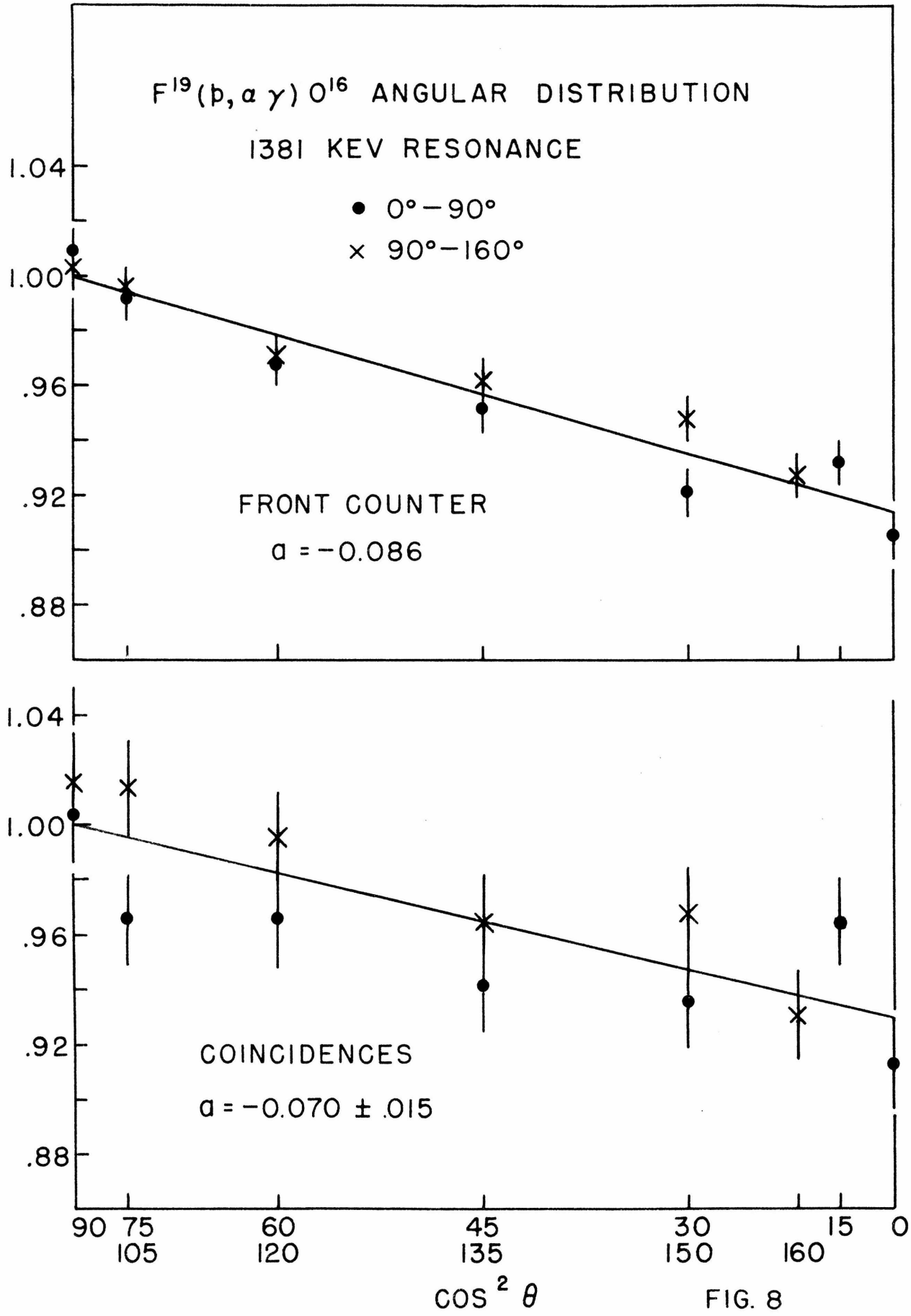
$F^{19}(p, \alpha\gamma)O^{16}$ ANGULAR DISTRIBUTION
1381 KEV RESONANCE
● 0°–90°
× 90°–160°
1.04
1.00
.96
.92
.88
FRONT COUNTER
a = −0.086
COINCIDENCES
a = −0.070 ± .015
90 75 60 45 30 15 0
105 120 135 150 160
$\cos^2\theta$

FIG. 8

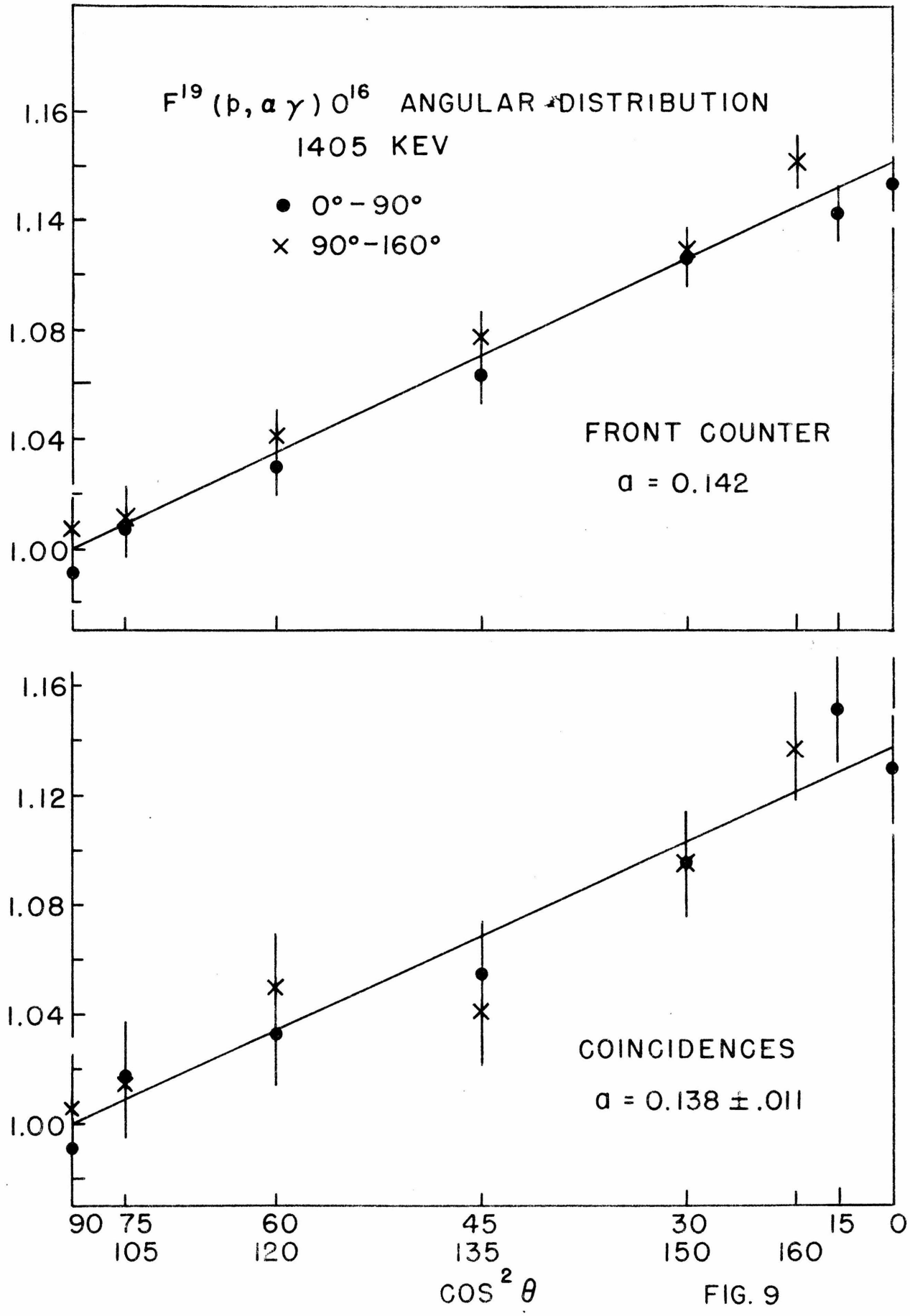
$F^{19}(p,\alpha\gamma)O^{16}$ ANGULAR DISTRIBUTION
1405 KEV
● 0°-90°
× 90°-160°
FRONT COUNTER
a = 0.142
COINCIDENCES
a = 0.138 ± .011
1.16
1.14
1.12
1.08
1.04
1.00
90 75 60 45 30 15 0
105 120 135 150 160
$\cos^2\theta$

FIG. 9

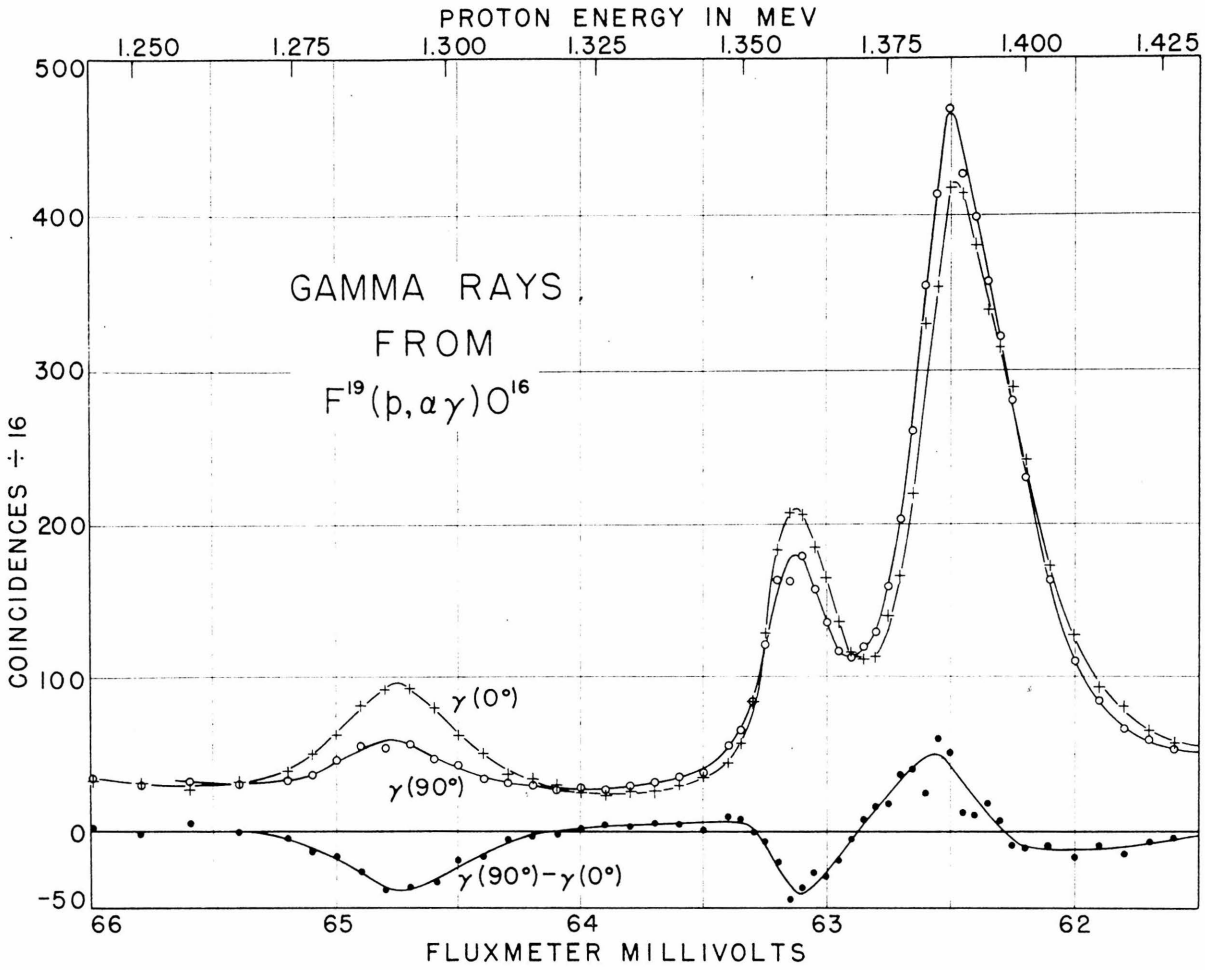
PROTON ENERGY IN MEV
1.250
1.275
1.300
1.325
1.350
1.375
1.400
1.425
500
400
300
200
100
0
-50
COINCIDENCES ÷ 16
GAMMA RAYS
FROM
$F^{19}(p,\alpha\gamma)O^{16}$
$\gamma(0°)$
$\gamma(90°)$
$\gamma(90°)-\gamma(0°)$
66
65
64
63
62
FLUXMETER MILLIVOLTS

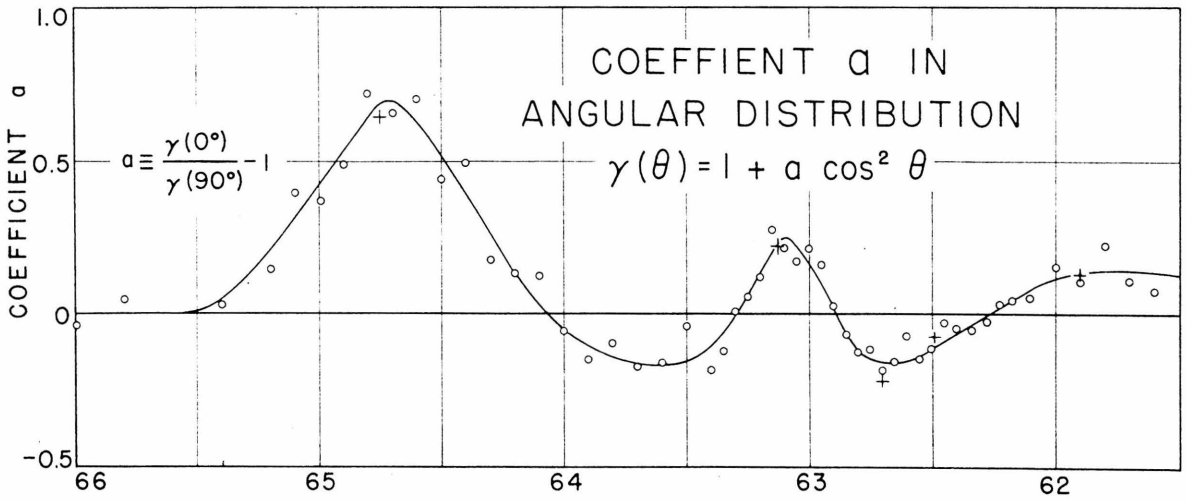
1.0
0.5
0
-0.5
COEFFICIENT a
$a \equiv \frac{\gamma(0°)}{\gamma(90°)} - 1$
COEFFIENT a IN
ANGULAR DISTRIBUTION
$\gamma(\theta) = 1 + a\cos^2\theta$
66
65
64
63
62

FIG. 10

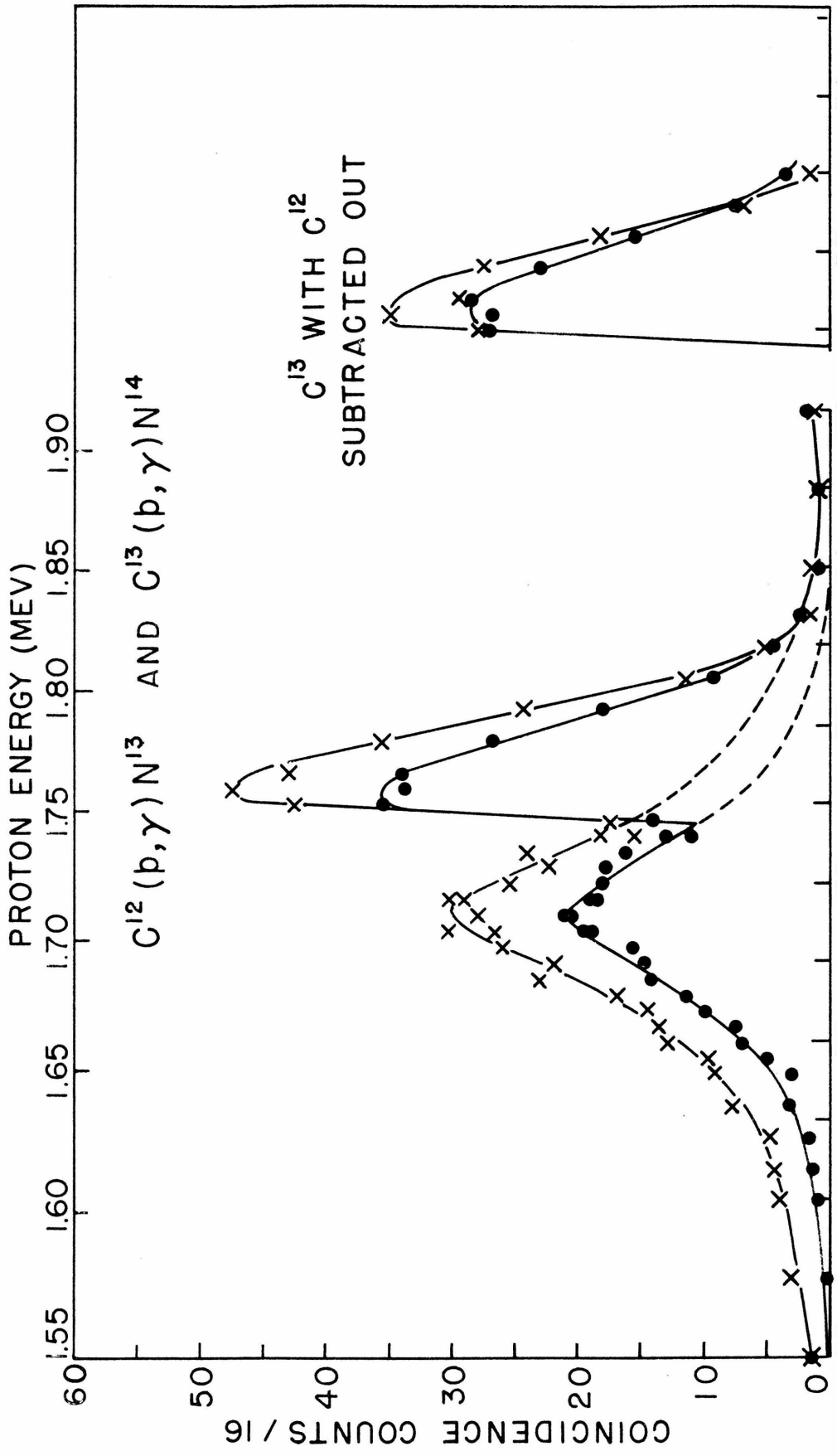
PROTON ENERGY (MEV)
1.55
1.60
1.65
1.70
1.75
1.80
1.85
1.90
$C^{12}(p,\gamma)N^{13}$ AND $C^{13}(p,\gamma)N^{14}$
C^{13} WITH C^{12} SUBTRACTED OUT
COINCIDENCE COUNTS / 16
0
10
20
30
40
50
60
MAGNETOMETER READING
53
54
55
56
57
58
59
54
55

FIG. 11

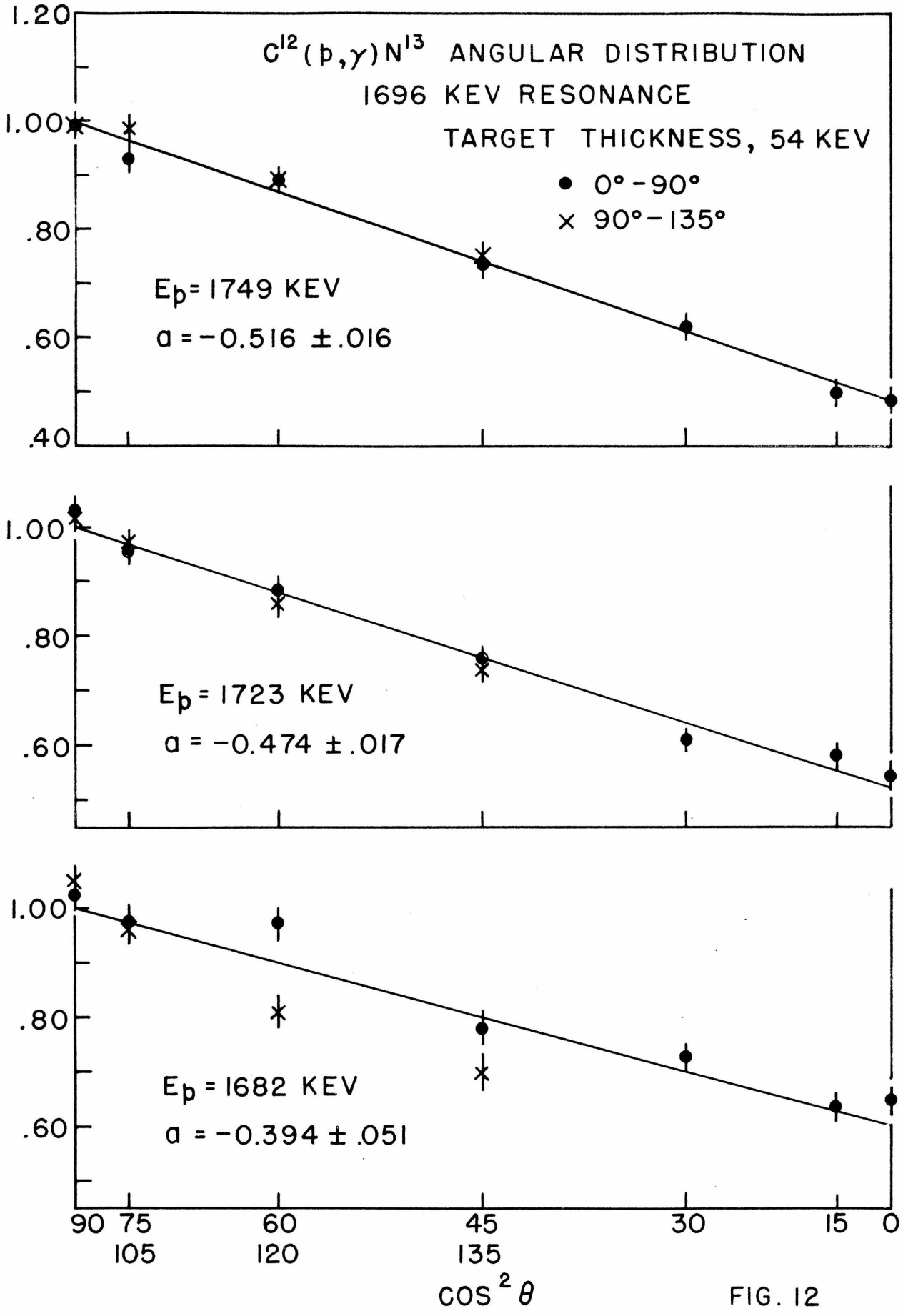
$C^{12}(p,\gamma)N^{13}$ ANGULAR DISTRIBUTION
1696 KEV RESONANCE
TARGET THICKNESS, 54 KEV
● 0°-90°
× 90°-135°
E_p= 1749 KEV
a = −0.516 ± .016
E_p = 1723 KEV
a = −0.474 ± .017
E_p = 1682 KEV
a = −0.394 ± .051
1.20
1.00
.80
.60
.40
90 75 60 45 30 15 0
105 120 135
$\cos^2\theta$

FIG. 12

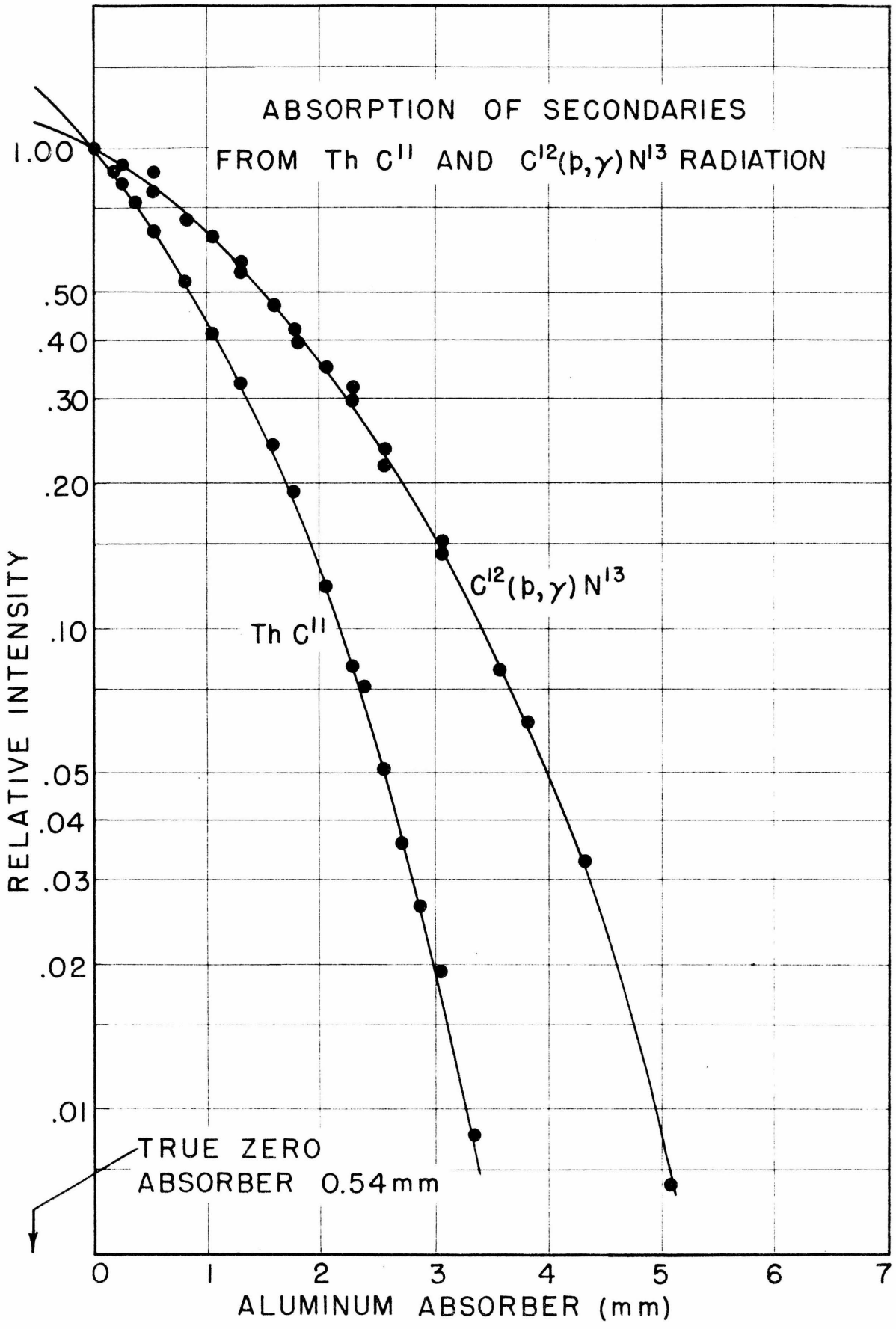
ABSORPTION OF SECONDARIES
FROM Th C11 AND C12(p,γ)N13 RADIATION
1.00
.50
.40
.30
.20
.10
.05
.04
.03
.02
.01
RELATIVE INTENSITY
C12(p,γ)N13
Th C11
TRUE ZERO
ABSORBER 0.54mm
0
1
2
3
4
5
6
7
ALUMINUM ABSORBER (mm)

FIG. 13

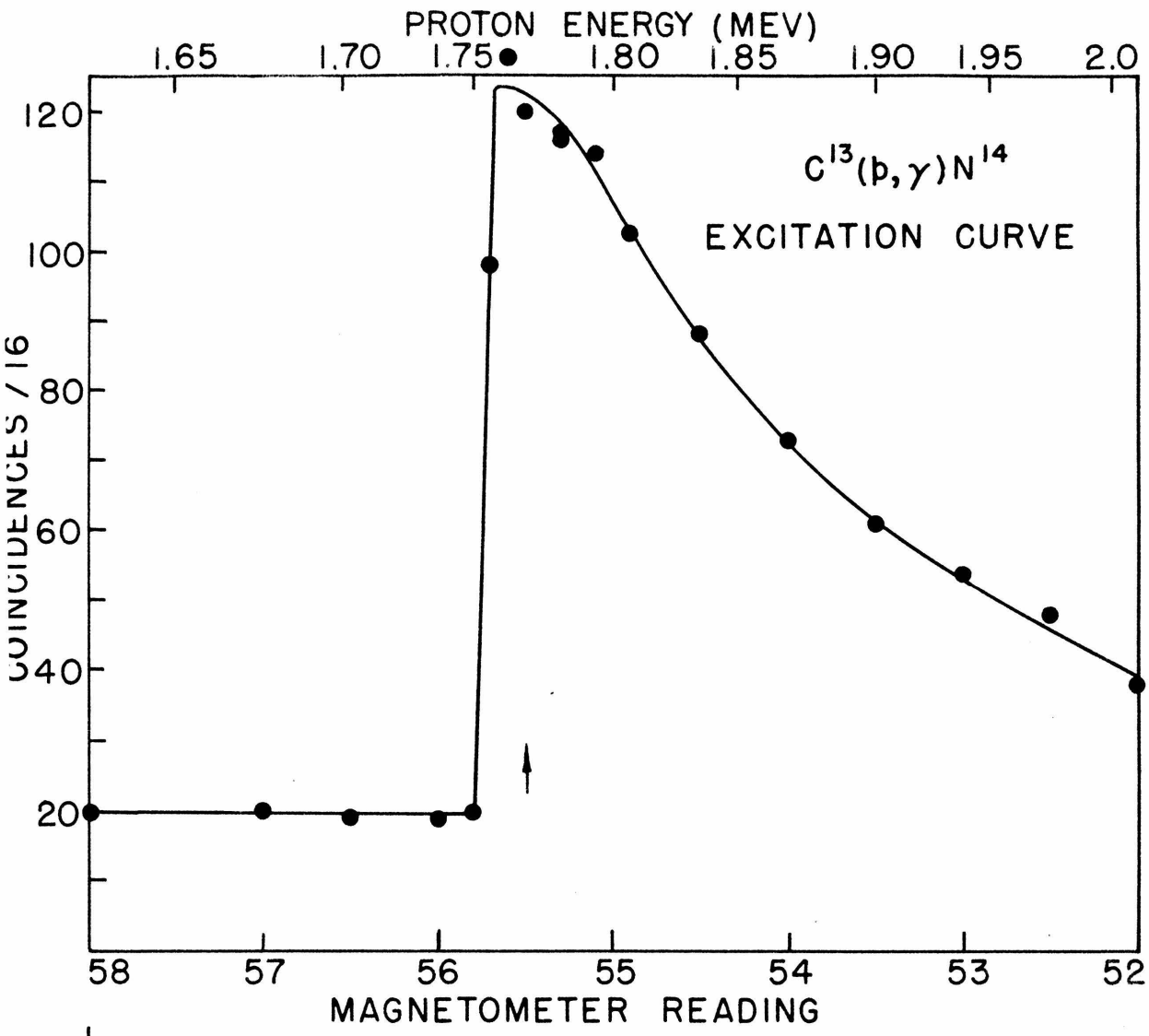
PROTON ENERGY (MEV)
1.65
1.70
1.75
1.80
1.85
1.90
1.95
2.0
120
100
80
60
40
20
COINCIDENCES / 16
$C^{13}(p,\gamma)N^{14}$
EXCITATION CURVE
58
57
56
55
54
53
52
MAGNETOMETER READING

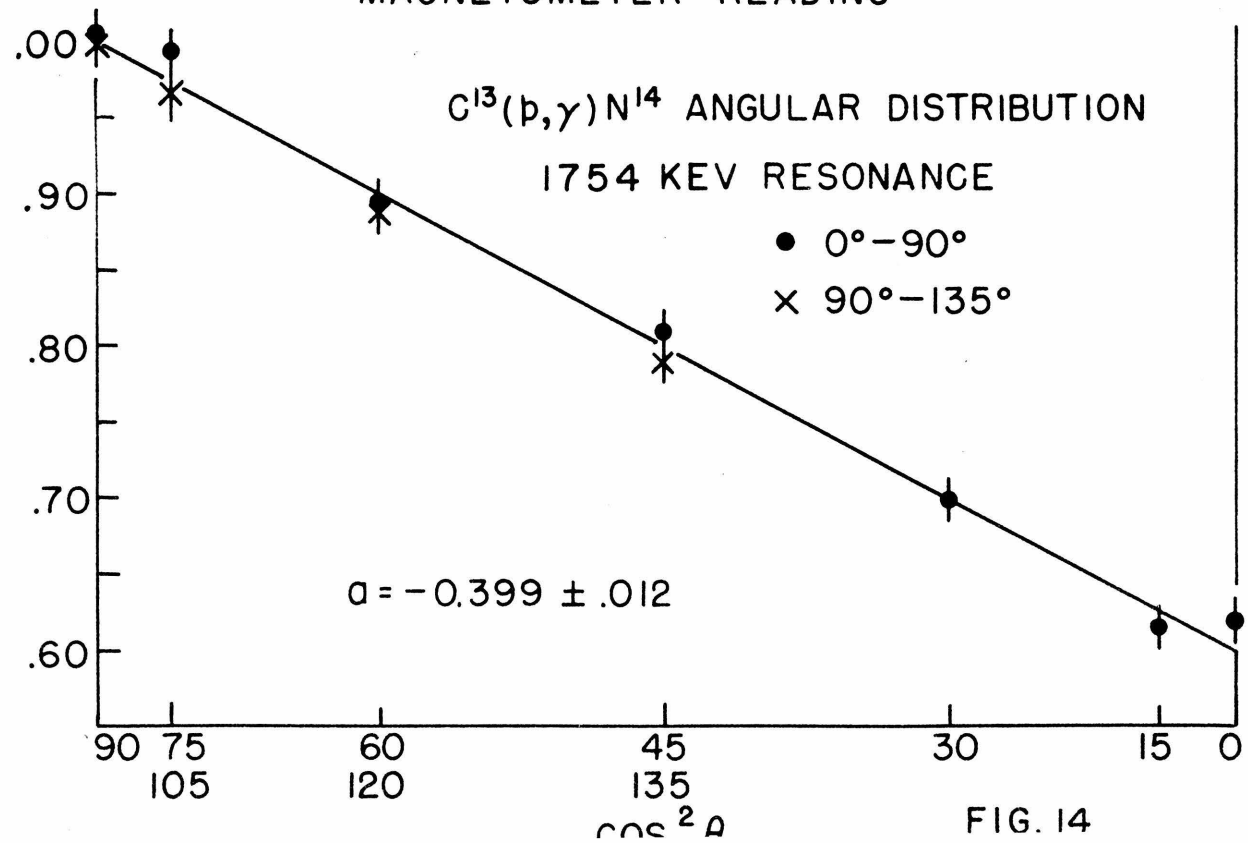
1.00
.90
.80
.70
.60
$C^{13}(p,\gamma)N^{14}$ ANGULAR DISTRIBUTION
1754 KEV RESONANCE
● 0°–90°
× 90°–135°
a = −0.399 ± .012
90
75
105
60
120
45
135
30
15
0
$\cos^2\theta$

FIG. 14